diseases; hence, further elucidation of their effects on each human eye is necessary. Based on this concept, the vitreous levels of VEGF, SDF-1α, interleukins (ILs), and tumor necrosis factor-α (TNF-α) were assessed after intravitreal injection of bevacizumab or TA in eyes with proliferative diabetic retinopathy (PDR), and the results showed that eyes with intravitreal bevacizumab had significantly lower levels of VEGF and SDF-1α than eyes without injection.

Patients and Methods

Study Population

A total of 47 eyes of 47 patients with type 2 diabetes who were affected by PDR were enrolled in this study. The patients were divided into 3 groups: an historical control of 18 consecutive patients received vitrectomy without preoperative therapy before January 2005 (control group), a second group of 10 consecutive patients receiving preoperative intravitreal TA operated on between February 2005 and April 2005 (TA group), and a third group of 19 consecutive patients receiving preoperative intravitreal bevacizumab operated on after February 2007 (bevacizumab group). The clinical histories of all patients were obtained from their medical records. Slit-lamp, funduscopic, fluorescein angiographic, and gonioscopic examinations were used to classify eyes as active PDR in which there was perfused retinal or iris neovascularization or both. To minimize individual variations, eyes with massive vitreous hemorrhage (in which the optic disc was invisible) or apparent tractional retinal detachment were excluded from the study group, and all patients had persistent diffuse macular edema detected by optical coherence tomography. All diagnoses were confirmed by at least 2 doctors independently at the time of admission. Bevacizumab (Avastin; Genentech, Inc., South San Francisco, CA; 1.25 mg/0.05 ml) or TA (Kenacort-A; Bristol-Myers Squibb Pharmaceuticals, Tokyo, Japan; 4 mg/0.1 ml) was injected into the vitreous cavity as preoperative adjunctive therapy 7 days before vitrectomy. Although there is no literature on the preoperative use of TA, it was reported that intravitreal TA possibly had an antiangiogenic effect on ocular neovascular diseases[4] and that VEGF and SDF-1 in eyes with diabetic retinopathy were eliminated 1 month after administration of 4 mg TA.[5] Therefore, the authors hypothesized that even 1 week of treatment with 4 mg TA could reduce these molecules to some extent and ameliorate the preoperative intraocular condition without an adverse event during in this therapeutic period. Based on this perspective, a pilot trial was conducted using TA as a preoperative adjunctive therapy before vitrectomy. All patients gave informed consent before treatment. All surgery was performed at Kagoshima University Hospital. This study was approved by the institutional ethical committee and was performed in accordance with the Declaration of Helsinki.

Sample Collection

For ethical and technical reasons, it was impossible to obtain paired samples of vitreous humors in the same eye (before and after injection). Therefore, only the vitreous humors of postinjection eyes were examined. Undiluted vitreous fluid samples (range, 0.5–0.7 ml) were obtained by pars plana vitrectomy. Vitreous humor was collected into sterile tubes, placed immediately on ice, centrifuged to remove cells and debris, and stored at −80°C until analysis.

Measurement of Vitreous Levels of Vascular Endothelial Growth Factor, Stromal Cell-Derived Factor 1α, Inflammatory Cytokines and Chemokines, and Total Protein

In this study, because of the limited amount of vitreous sampling, 2 different techniques, enzyme-linked immunosorbent assays (ELISAs) and a multiplex cytometric bead array (CBA) technology, were used for determining the vitreous levels of 8 molecules from the same samples, according to a previously described method.[7] Although the absolute value in CBA technology can differ from the ELISA value, it was reported that the concentrations follow similar patterns among kits from multiple suppliers.[8] Measurements obtained by ELISAs and CBA technologies also were confirmed to be highly correlated in vitreous samples.[9] Therefore, this method was considered to be applicable to the following statistical analyses.

Vascular endothelial growth factor and SDF-1α were quantified in each sample using commercial ELISAs: human VEGF and CXCL12/SDF-1α immunoassays (R&D Systems, Minneapolis, MN). Each assay was performed in duplicate according to the manufacturer's instructions and used a 50-μl vitreous sample (prediluted to 100 μl) per well for the VEGF ELISA and 100 μl (without predilution) for the SDF-1α ELISA. In this setting, the detection limits were 18 pg/ml for both VEGF and SDF-1α ELISAs.

Interleukin-1β, IL-6, IL-8, IL-10, IL-12p70, and TNF-α were quantified using a commercial multiplex CBA system, Human Inflammation Kit (BD Biosciences Pharmingen, San Diego, CA), according to the manufacturer's protocols. The sample requirement was 50 μl; therefore, undiluted 50-μl vitreous samples were used for the CBA kit. The detection limits for IL-1β, IL-6, IL-8, IL-10, IL-12p70, and TNF-α were 7.2, 2.5, 3.6, 3.3, 1.9, and 3.7 pg/ml, respectively. All concentrations less than the detection level were assigned a value of 0 in the subsequent analysis.

Total protein (TP) concentration was determined using a microbicinchoninic acid protein assay reagent (Pierce Biotechnology, Rockford, IL) according to the manufacturer's protocols. It is well known that vitreous protein concentration is increased by serum diffusion because of the breakdown of the blood–retinal barrier in eyes with PDR and potentially contributes to the increase of intravitreous VEGF and other mediators. To avoid the influence of serum diffusion, the authors believed it necessary to measure the protein concentration, and then the results were expressed as ratios of concentration to TP (pg/mg) as well as concentrations (pg/ml), as previous described.[10]

Statistical Analysis

Because of the skewed distribution, results were analyzed statistically using nonparametric tests (Kruskal-Wallis variance analysis and Mann–Whitney U test) and were expressed as median and range. Kruskal-Wallis variance analysis was performed to assess differences among the bevacizumab, TA, and control groups for the levels of all molecules. This was followed by pairwise comparisons using the Mann–Whitney U test. Statistical analyses were performed using SPSS software version 16.0 (SPSS, Inc., Chicago, IL). A P value $<.05$ was considered to be statistically significant. To adjust for inflated α error resulting from multiple comparisons, the corrected significant P value was defined as 0.05/3 using the Bonferroni correction for multiple comparisons.

Because no changes in the significances were found after excluding all potential outliers identified on the basis of the standard 1.5 interquartile range rule and used nonparametric tests, which are less sensitive to distribution parameters including outliers, all values including potential outliers were used for the statistical analyses.

Table 1. Characteristics of the Patients

Characteristic	Bevacizumab (n = 19)	Triamcinolone Acetonide (n = 10)	Control (n = 18)	*P* Value
Age (yrs)	54 (41–72)	55 (47–70)	62 (36–75)	0.079*
Female gender, no. (%)	5 (26)	3 (30)	10 (56)	0.156†
Duration of diabetes (yrs)	11 (6–32)	13 (10–30)	15 (6–40)	0.278*
Hemoglobin A1c (%)	7.95 (5.5–10.6)	7.1 (5.7–9.1)	7.3 (6.0–11.6)	0.770*
Hypertensive, no. (%)	11 (58)	5 (50)	11 (61)	0.849†
PRP, no. (%)	12 (63)	8 (80)	15 (83)	0.336†
Period from last PRP to vitrectomy (mos)	5 (2.5–84)	11 (5–48)	11 (2–96)	0.417*

PRP = panretinal photocoagulation.
Values are expressed as median (range) or number (%).
*Kruskal-Wallis variance analysis.
†Chi-square test.

Results

The baseline characteristics of each group are summarized in Table 1. There was no statistical significance in age, gender, duration of diabetes, hemoglobin A1c, and hypertension. In particular, the ratio and the timing of previous panretinal photocoagulation, which may alter the levels of VEGF and other mediators at the time of surgery and may contribute to the wide ranges of values for these intravitreous molecules, were not significantly different among the 3 groups (Table 1).

Between intravitreal injection and vitrectomy, no complications, such as uveitis, endophthalmitis, tractional retinal detachment, ocular hypertension, or any obvious ocular or systemic adverse events developed in any eyes. Although there were some variations, all eyes with intravitreal bevacizumab or TA showed similar tendencies of decreases of fluorescein leakage on angiogram and reduction of central macular thickness on optical coherence tomography after vitrectomy. However, no significant differences in retinal thickness measured by optical coherence tomography could be found among the 3 groups, and there were no apparent correlations between the low level of VEGF and the reduction of macular edema (data not shown).

Table 2 shows concentrations of vitreous VEGF, SDF-1α, ILs, and TNF-α in the bevacizumab, TA, and control groups. Significant differences among the 3 groups were observed for the levels of VEGF and SDF-1α ($P<0.001$ and $P = 0.010$, respectively), which also were noted after normalization to total vitreous protein concentration ($P<0.001$ and $P = 0.018$, respectively; Table 3).

Vascular Endothelial Growth Factor Levels

The median VEGF level was 0 pg/ml (range, 0–79.2 pg/ml) in the bevacizumab group, 343.5 pg/ml (range, 0–1683.3 pg/ml) in the TA group, and 1202.5 pg/ml (range, 76–4213.9 pg/ml) in the control group (Table 2). The eyes with intravitreal bevacizumab had the lowest vitreous level of VEGF, and the level was statistically significant compared with that of eyes with intravitreal TA and that of the control eyes ($P<0.001$ and $P<0.001$, respectively; Fig 1A). This trend continued after normalization to TP (Table 3 and Fig 1B). In addition, the median vitreous VEGF concentration was lower in eyes with intravitreal TA than those without injection ($P = 0.049$; Fig 1A). However, this is not statistically significant in consideration of Bonferroni correction, as well as when the levels were normalized to TP concentrations ($P = 0.150$; Fig 1B).

Stromal Cell-Derived Factor 1α Levels

The median SDF-1α level was 149.2 pg/ml (range, 0–519.4 pg/ml) in the bevacizumab group, 87.5 pg/ml (range, 0–252.5 pg/ml) in the TA group, and 245.7 pg/ml (range, 0–856.8 pg/ml) in the control group (Table 2). The control eyes had the highest vitreous

Table 2. Comparison of Median Vitreous Concentrations in Bevacizumab, Triamcinolone Acetonide, and Control Groups

	Bevacizumab (n = 19)	Triamcinolone Acetonide (n = 10)	Control (n = 18)	*P* Value*
VEGF	0 (0–79.2)	343.5 (0–1683.3)	1202.5 (76–4213.9)	<0.001‡
SDF-1α	149.2 (0–519.4)	87.5 (0–252.5)	245.7 (0–856.8)	0.010†
IL-1β	0 (0–104.7)	0 (0–60.8)	15.7 (0–115.3)	0.176
IL-6	66.9 (10.2–723.8)	58.1 (3.4–507.5)	86.3 (3.5–457.6)	0.916
IL-8	69.5 (14.1–1131.3)	92.6 (0–254.9)	63.1 (5.3–726.7)	0.890
IL-10	0 (0–14.2)	0 (0–13.5)	0 (0–8)	0.810
IL-12p70	4.8 (0–28.7)	2 (0–13.4)	4.2 (0–26.9)	0.781
TNF-α	0 (0–17.7)	0 (0–12.5)	0 (0–12)	0.478

IL = interleukin; SDF = stromal cell-derived factor; TNF = tumor necrosis factor; VEGF = vascular endothelial growth factor.
Values are expressed as median and range (pg/ml).
*Kruskal-Wallis variance analysis for bevacizumab, triamcinolone acetonide, and control groups.
†$P<0.05$.
‡$P<0.01$.

Table 3. Comparison of Median Vitreous Levels (Normalized to Total Protein) in Bevacizumab, Triamcinolone Acetonide, and Control Groups

	Bevacizumab (n = 19)	Triamcinolone Acetonide (n = 10)	Control (n = 18)	P Value*
VEGF/TP	0 (0–23.2)	174.5 (0–383)	300.1 (13.8–1427.1)	<0.001‡
SDF-1α/TP	37.7 (0–69.4)	31.1 (0–177.6)	60.8 (0–213.8)	0.018†
IL-1β/TP	0 (0–46.2)	0 (0–42.8)	4.3 (0–41.3)	0.360
IL-6/TP	25.8 (1.3–205.4)	30.2 (5.0–356.9)	17.2 (1.2–114.2)	0.793
IL-8/TP	23.9 (6.8–169.2)	23.5 (0–179.3)	15.2 (2.4–209.5)	0.459
IL-10/TP	0 (0–5.3)	0 (0–9.5)	0 (0–2.9)	0.823
IL-12p70/TP	0.9 (0–25.5)	0.8 (0–9.4)	1.5 (0–5.9)	0.983
TNF-α/TP	0 (0–10.5)	0 (0–8.8)	0 (0–4.4)	0.705

IL = interleukin; SDF = stromal cell-derived factor; TNF = tumor necrosis factor; TP = total protein; VEGF = vascular endothelial growth factor.
Vitreous concentrations in Table 1 are normalized to TP concentration.
Values are expressed as median and range (pg/mg).
*Kruskal-Wallis variance analysis for bevacizumab, triamcinolone acetonide, and control groups.
†$P<0.05$.
‡$P<0.01$.

level of SDF-1α, and the level was statistically significant compared with eyes with intravitreal bevacizumab and TA ($P = 0.015$ and $P = 0.009$, respectively; Fig 2A). The difference in the median ratio of SDF-1α to TP (SDF-1α/TP) also was statistically significant between the control and bevacizumab groups ($P = 0.007$; Fig 2B). In contrast, the difference in the SDF-1α-to-TP ratio between the control and the TA groups was not statistically significant ($P = 0.054$). There were no significant differences between bevacizumab and TA groups in either SDF-1α concentration or SDF-1α-to-TP ratio.

Interleukin and Tumor Necrosis Factor-α Levels

There was no significant differences regarding ILs and TNF-α at both concentrations (pg/ml; Table 2) or at ratios of concentration to TP (pg/mg; Table 3).

Discussion

A growing number of studies indicate that intravitreal injection of bevacizumab improves the clinical conditions of ocular neovascular disorders resulting from the blockade of VEGF.[2,3,11] Sawada et al[6] clearly showed that VEGF in the aqueous humor decreased substantially after intravitreal injection of bevacizumab. The current results for vitreous humor are comparable with those of that report. It was also presented in the experimental study using rabbits by Bakri et al[12] that vitreous concentrations of bevacizumab declined in a monoexponential fashion with a half-life of 4.32 days, and relatively high concentrations of bevacizumab were maintained in the vitreous humor for 30 days. According to this report, bevacizumab is supposed to be present in the vitreous at the time of vitrectomy, 7 days after intravitreal injection. Therefore, there are 2 possibilities: VEGF is not present (disappearance of VEGF) or the epitope of VEGF, detectable by the antibody used in the ELISA, is masked by bevacizumab (presence of VEGF–bevacizumab complex; undetectable by ELISA). Because whether the VEGF–bevacizumab complex actually existed was not addressed, the values of VEGF that were less than the detection level in the bevacizumab group were assigned as 0 by referring to a previous report.[6]

This study found that SDF-1α also is potentially influenced by bevacizumab. Stromal cell-derived factor 1 is the predominant chemokine that traffics hematopoietic and endothelial progenitor cells to promote not only physiologic vascular remodeling for development and wound healing, but also pathologic vascular remodeling for ocular neovascular diseases and tumor growth.[13,14] Recently, increases in vitreous SDF-1α levels in eyes with diabetic retinopathy,[5] retinal vein occlusion,[7] and retinopathy of prematurity[10] have been reported, and its essential role for ocular pathologic neovascularization also has been confirmed using experimental animal models.[15,16] Although there is no published information available concerning the regulation of SDF-1 expression in ocular fluid, Grunewald et al[17] reported that locally expressed VEGF mobilizes and recruits bone marrow-derived cells via SDF-1 and that SDF-1 expression is augmented in activated perivascular myofibroblasts of heart, liver, and skin in a VEGF-dependent manner. In ocular tissue, SDF-1 was reported to be expressed by ischemic astrocytes in mice.[16] Therefore, it is possible that intraocular SDF-1 was upregulated by VEGF in a similar way in eyes with PDR and that the blockade of VEGF by bevacizumab resulted in downregulation of SDF-1.

The observation that concentrations of VEGF and SDF-1α also were low in samples collected after injection of TA is compatible with the previous report.[5,15] Triamcinolone acetonide is one of the corticosteroids known to inhibit the production of several proangiogenic and inflammatory mediators by both transcriptional and posttranscriptional mechanisms.[18,19] In addition, inflammation has been thought to enhance the effects of VEGF further.[20] As a result, TA may decrease the levels of VEGF and SDF-1 in the vitreous fluid. However, it is interesting that the ratios of both VEGF and SDF-1α to TP are not significantly lower in the TA group than in the control group in this study, which may be the result of the marked reduction of serum diffusion caused by intravitreal TA administration. In contrast, it is difficult to assess the influence of TP in eyes with intravitreal bevacizumab, because bevacizumab is itself a protein and TP

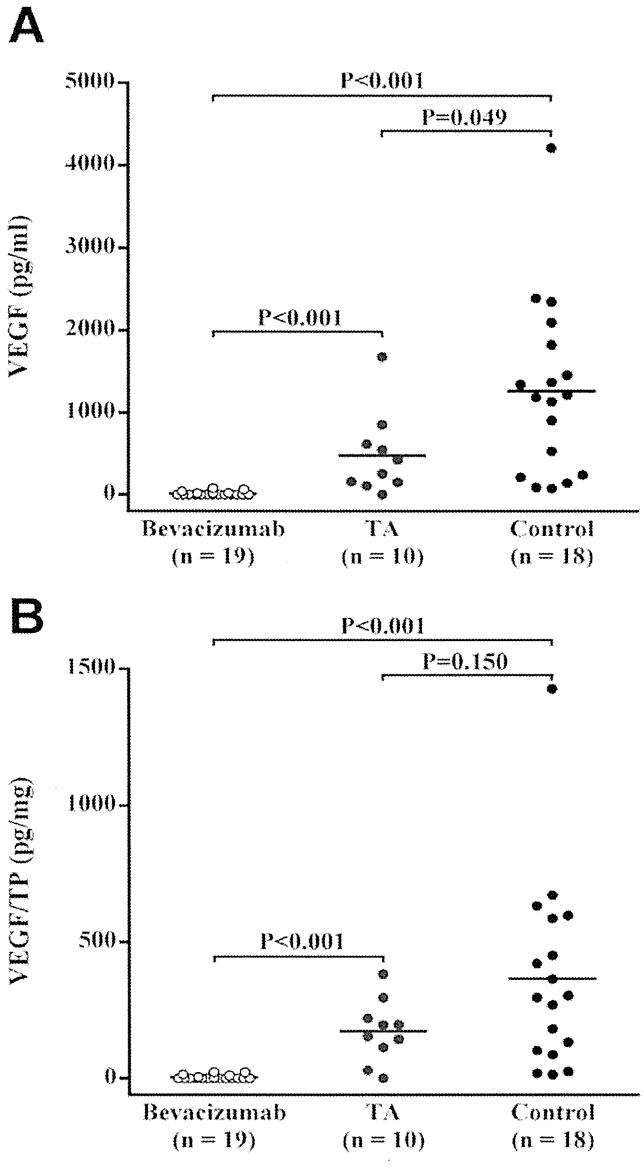

Figure 1. A, Graph demonstrating vascular endothelial growth factor (VEGF) levels in the vitreous fluid of subjects with intravitreal bevacizumab (white circles), triamcinolone acetonide (TA; gray circles), and without injection (control; black circles). B, Graph demonstrating ratios of VEGF to vitreous total protein concentration. Each bar indicates the average value. The corrected significant *P* value (Mann–Whitney *U* test) was defined as 0.02 (0.05/3 comparisons) after Bonferroni correction. TP = total protein.

must be increased by bevacizumab injection, which may offset the potential reduction of serum diffusion caused by intravitreal bevacizumab administration at the same time.

Although it was postulated that bevacizumab and TA may alter the ocular inflammatory context, there was no significant difference with regard to ILs and TNF-α. The results for the bevacizumab-injected eyes indicate that these mediators may not be regulated by VEGF. The data from the TA-injected eyes also showed similar results. Triamcinolone acetonide should decrease these inflammatory mediators in theory,[21] but the results suggest no reductions of these molecules as opposed to VEGF and SDF-1α. Further studies may be needed to determine how these intraocular mediators are affected by these treatments.

Nevertheless, it is of note that the results for bevacizumab gave much clearer evidence than did those for TA. Although the knockout animal study has contributed greatly to a better understanding of the role of specific molecules in various diseases, the information obtained by the knockout animal study is just that for animals, and has to be interpreted carefully before being generalized to human diseases. Knockout technology can never be applied to human beings for ethical reasons. However, the present treatment based on antibody-drug technology could produce a so-called knock-

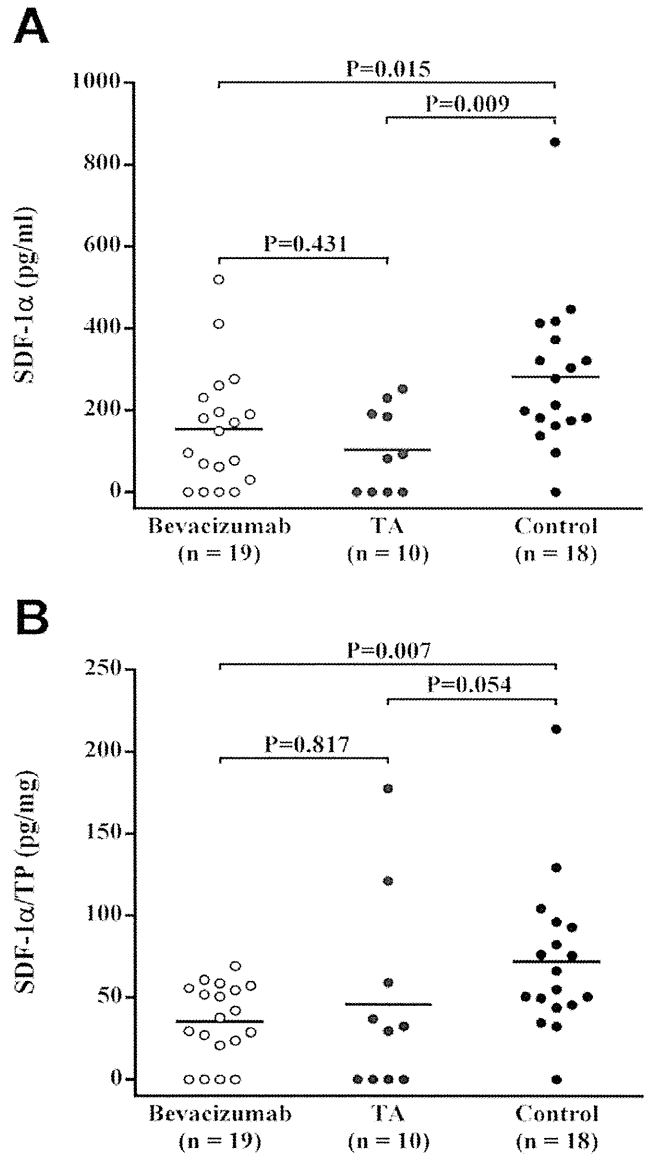

Figure 2. A, Graph demonstrating stromal cell-derived factor 1α (SDF-1α) levels in the vitreous fluid of subjects with intravitreal bevacizumab (white circles), triamcinolone acetonide (TA; gray circles), and without injection (control; black circles). B, Graph demonstrating ratios of SDF-1α to vitreous total protein concentration. Each bar indicates the average value. The corrected significant *P* value (Mann–Whitney *U* test) was defined as 0.02 (0.05/3 comparisons) after Bonferroni correction. TP = total protein.

out condition in humans without raising ethical problems. For example, the present result for bevacizumab showed direct evidence that intravitreous SDF-1 potentially is affected by VEGF in PDR, which cannot be achieved by previous technology. This concept, which is called interventional immunology by Hafler,[22] will generate more important information on various human diseases in the future.

This was a retrospective, comparative study, and the comparisons are based on historical controls. Although the use of a preoperative drug was not determined based on ocular condition, but rather on surgical period and the background of each group matched well, there is a possibility of selection bias making a definitive conclusion difficult. A further prospective study that includes a randomized design may be needed to confirm the present findings.

In conclusion, bevacizumab can downregulate SDF-1α via the blockade of VEGF, and this treatment may have broader and more profound influences on ocular tissue than has been thought. Further study of this treatment is recommended.

References

1. Folkman J. Angiogenesis: an organizing principle for drug discovery? Nat Rev Drug Discov 2007;6:273–86.
2. Avery RL, Pieramici DJ, Rabena MD, et al. Intravitreal bevacizumab (Avastin) for neovascular age-related macular degeneration. Ophthalmology 2006;113:363–72.
3. Arevalo JF, Fromow-Guerra J, Quiroz-Mercado H, et al, Pan-American Collaborative Retina Study Group. Primary intravitreal bevacizumab (Avastin) for diabetic macular edema: results from the Pan-American Collaborative Retina Study Group at 6-month follow-up. Ophthalmology 2007;114:743–50.
4. Jonas JB, Kreissig I, Degenring R. Intravitreal triamcinolone acetonide for treatment of intraocular proliferative, exudative, and neovascular diseases. Prog Retin Eye Res 2005;24:587–611.
5. Brooks HL Jr, Caballero S Jr, Newell CK, et al. Vitreous levels of vascular endothelial growth factor and stromal-derived factor 1 in patients with diabetic retinopathy and cystoid macular edema before and after intraocular injection of triamcinolone. Arch Ophthalmol 2004;122:1801–7.
6. Sawada O, Kawamura H, Kakinoki M, et al. Vascular endothelial growth factor in aqueous humor before and after intravitreal injection of bevacizumab in eyes with diabetic retinopathy. Arch Ophthalmol 2007;125:1363–6.
7. Ki-I Y, Arimura N, Noda Y, et al. Stromal-derived factor-1 and inflammatory cytokines in retinal vein occlusion. Curr Eye Res 2007;32:1065–72.
8. Khan SS, Smith MS, Reda D, et al. Multiplex bead array assays for detection of soluble cytokines: comparisons of sensitivity and quantitative values among kits from multiple manufacturers. Cytometry B Clin Cytom 2004;61:35–9.
9. Maier R, Weger M, Haller-Schober EM, et al. Application of multiplex cytometric bead array technology for the measurement of angiogenic factors in the vitreous. Mol Vis 2006;12:1143–7.
10. Sonmez K, Drenser KA, Capone A Jr, Trese MT. Vitreous levels of stromal cell-derived factor 1 and vascular endothelial growth factor in patients with retinopathy of prematurity. Ophthalmology 2008;115:1065–70.
11. Avery RL, Pearlman J, Pieramici DJ, et al. Intravitreal bevacizumab (Avastin) in the treatment of proliferative diabetic retinopathy. Ophthalmology 2006;113:1695–705.
12. Bakri SJ, Snyder MR, Reid JM, et al. Pharmacokinetics of intravitreal bevacizumab (Avastin). Ophthalmology 2007;114:855–9.
13. Grant MB, May WS, Caballero S, et al. Adult hematopoietic stem cells provide functional hemangioblast activity during retinal neovascularization. Nat Med 2002;8:607–12.
14. Ratajczak MZ, Zuba-Surma E, Kucia M, et al. The pleiotropic effects of the SDF-1-CXCR4 axis in organogenesis, regeneration and tumorigenesis. Leukemia 2006;20:1915–24.
15. Butler JM, Guthrie SM, Koc M, et al. SDF-1 is both necessary and sufficient to promote proliferative retinopathy. J Clin Invest 2005;115:86–93.
16. Lima e Silva R, Shen J, Hackett SF, et al. The SDF-1/CXCR4 ligand/receptor pair is an important contributor to several types of ocular neovascularization. FASEB J 2007;21:3219–30.
17. Grunewald M, Avraham I, Dor Y, et al. VEGF-induced adult neovascularization: recruitment, retention, and role of accessory cells. Cell 2006;124:175–89.
18. Mukaida N, Morita M, Ishikawa Y, et al. Novel mechanism of glucocorticoid-mediated gene repression: nuclear factor-kappa B is target for glucocorticoid-mediated interleukin 8 gene repression. J Biol Chem 1994;269:13289–95.
19. Nie M, Corbett L, Knox AJ, Pang L. Differential regulation of chemokine expression by peroxisome proliferator-activated receptor gamma agonists: interactions with glucocorticoids and beta2-agonists. J Biol Chem 2005;280:2550–61.
20. Adamis AP. Is diabetic retinopathy an inflammatory disease? Br J Ophthalmol 2002;86:363–5.
21. Jaffuel D, Demoly P, Gougat C, et al. Transcriptional potencies of inhaled glucocorticoids. Am J Respir Crit Care Med 2000;162:57–63.
22. Hafler DA. Cytokines and interventional immunology. Nat Rev Immunol 2007;7:423.

Footnotes and Financial Disclosures

Originally received: April 10, 2008.
Final revision: September 11, 2008.
Accepted: December 1, 2008. Manuscript no. 2008-453.

[1] Department of Ophthalmology, Kagoshima University Graduate School of Medical and Dental Sciences, Kagoshima, Japan.

[2] Department of Ophthalmology, Graduate School of Medical Sciences, Kyushu University, Fukuoka, Japan.

[3] Department of Laboratory and Vascular Medicine, Kagoshima University Graduate School of Medical and Dental Sciences, Kagoshima, Japan.

Presented at: Association for Research in Vision and Ophthalmology Annual Meeting, May 2008; Fort Lauderdale, Florida.

Financial Disclosure(s):
The author(s) have no proprietary or commercial interest in any materials discussed in this article.

Supported in part by a grant from the Research Committee on Chorioretinal Degeneration and Optic Atrophy, Ministry of Health, Labor, and Welfare, Tokyo, Japan; and by a Grant-in-Aid for Scientific Research from the Ministry of Education, Science, and Culture of the Japanese Government, Tokyo, Japan.

Correspondence:
Taiji Sakamoto, MD, PhD, Department of Ophthalmology, Kagoshima University Graduate School of Medical and Dental Sciences, 8-35-1, Sakuragaoka, Kagoshima 890-8520, Japan. E-mail: tsakamot@m3.kufm.kagoshima-u.ac.jp.

Laboratory Investigation (2009) 89, 278–289

Intraocular expression and release of high-mobility group box 1 protein in retinal detachment

Noboru Arimura[1,2], Yuya Ki-i[1,2], Teruto Hashiguchi[2], Ko-ichi Kawahara[2], Kamal K Biswas[2], Makoto Nakamura[3], Yasushi Sonoda[1], Keita Yamakiri[1], Akiko Okubo[1], Taiji Sakamoto[1] and Ikuro Maruyama[2]

High-mobility group box 1 (HMGB1) protein is a multifunctional protein, which is mainly present in the nucleus and is released extracellularly by dying cells and/or activated immune cells. Although extracellular HMGB1 is thought to be a typical danger signal of tissue damage and is implicated in diverse diseases, its relevance to ocular diseases is mostly unknown. To determine whether HMGB1 contributes to the pathogenesis of retinal detachment (RD), which involves photoreceptor degeneration, we investigated the expression and release of HMGB1 both in a retinal cell death induced by excessive oxidative stress *in vitro* and in a rat model of RD-induced photoreceptor degeneration *in vivo*. In addition, we assessed the vitreous concentrations of HMGB1 and monocyte chemoattractant protein 1 (MCP-1) in human eyes with RD. We also explored the chemotactic activity of recombinant HMGB1 in a human retinal pigment epithelial (RPE) cell line. The results show that the nuclear HMGB1 in the retinal cell is augmented by death stress and upregulation appears to be required for cell survival, whereas extracellular release of HMGB1 is evident not only in retinal cell death *in vitro* but also in the rat model of RD *in vivo*. Furthermore, the vitreous level of HMGB1 is significantly increased and is correlated with that of MCP-1 in human eyes with RD. Recombinant HMGB1 induced RPE cell migration through an extracellular signal-regulated kinase-dependent mechanism *in vitro*. Our findings suggest that HMGB1 is a crucial nuclear protein and is released as a danger signal of retinal tissue damage. Extracellular HMGB1 might be an important mediator in RD, potentially acting as a chemotactic factor for RPE cell migration that would lead to an ocular pathological wound-healing response.

Laboratory Investigation (2009) **89,** 278–289; doi:10.1038/labinvest.2008.165; published online 12 January 2009

KEYWORDS: danger signal; high-mobility group box 1 protein; photoreceptor degeneration; retinal detachment; tissue damage; wound healing

Cell death is the predominant event of degenerative tissue damage and can be a trigger that activates the immune system and repair program. Recently, there has been much interest in the pivotal role of endogenous danger signals released during cell death.[1] High-mobility group box 1 (HMGB1) protein is a prototypic innate danger signal, and appears to be crucial in this context because extracellular HMGB1 [2] can modulate inflammation, proliferation, and remodeling, which are involved in the wound-healing process.[3]

HMGB1 was originally described as an abundant and ubiquitous nuclear DNA-binding protein that had multiple functions dependent on its cellular location.[2,4] In the nucleus, HMGB1 binds to DNA and is critical for proper transcriptional regulation. It is also called amphoterin and accelerates cellular motility on the cell surface.[5] HMGB1 is reported to be passively released into the extracellular milieu by necrotic cells, but not by apoptotic cells,[6] or is exported actively by monocytes/macrophages[7] and neural cells[8] upon receiving appropriate stimuli. In damaged tissue, extracellular HMGB1 acts as a necrotic signal, which alerts the surrounding cells and the immune system.[2] Although extracellular HMGB1 can contribute to normal tissue development and repair, it is also implicated in the pathogenesis of several diseases (including lethal endotoxemia,[7] disseminated intravascular coagulation,[9] ischemic brain,[10] tumor,[11] atherosclerosis,[12] rheumatoid arthritis,[13] and periodontitis[14]).

[1]Department of Ophthalmology, Kagoshima University Graduate School of Medical and Dental Sciences, Kagoshima, Japan; [2]Department of Laboratory and Vascular Medicine, Kagoshima University Graduate School of Medical and Dental Sciences, Kagoshima, Japan and [3]Division of Ophthalmology, Department of Surgery, Kobe University Graduate School of Medicine, Kobe, Japan
Correspondence: Professor T Sakamoto, MD, PhD, Department of Ophthalmology, Kagoshima University Graduate School of Medical and Dental Sciences, 8-35-1, Sakuragaoka, Kagoshima 890-8520, Japan.
E-mail: tsakamot@m3.kufm.kagoshima-u.ac.jp

Received 25 August 2008; revised 9 October 2008; accepted 13 October 2008

Retinal detachment (RD), the physical separation of photoreceptors from the underlying retinal pigment epithelium (RPE), is one of the main causes of visual loss. Photoreceptor degeneration due to RD is thought to be executed by apoptosis[15,16] and necrosis,[17] which usually occur after tissue damage. Although retinal cell death and the following reactive responses must occur in almost all forms of retinal disease including RD,[18] data regarding the relationship among cell death, danger, and responses in the eye, have been very limited, especially in terms of danger signals. We previously reported that HMGB1 was significantly elevated in inflamed eyes with endophthalmitis, and suggested a possible link between HMGB1 and ocular inflammatory diseases.[19] On the other hand, considering the properties of HMGB1, we hypothesized that HMGB1 might have some roles in photoreceptor degeneration and subsequent damage-associated reactions in RD.

To investigate whether HMGB1 is involved in the pathogenesis of RD, we first examined the expression and release of HMGB1 both in a retinal cell death *in vitro* and in a rat model of RD-induced photoreceptor degeneration *in vivo*. To focus on human RD, we assessed the intravitreous concentrations of HMGB1 in human eyes affected by RD. Monocyte chemoattractant protein 1 (MCP-1), which was recently documented to be a potential proapoptotic mediator in RD,[20] was also measured in the same vitreous samples. We further analyzed the effects of recombinant HMGB1 (rHMGB1) on chemotactic activity in a RPE cell line *in vitro*. Our findings suggest that extracellular HMGB1 is evident in eyes with RD as a danger signal, potentially acting as a chemotactic factor for RPE cell migration that would lead to ocular pathological wound healing.

MATERIALS AND METHODS

Reagents

Full-length, LPS-free rat rHMGB1 protein, which is 99% identical to human HMGB1 and is fully functional on cells of mammalian origin,[21] was purchased from HMGBiotech (Milan, Italy). Human recombinant MCP-1 (rMCP-1) was purchased from Peprotec (Rocky Hill, NJ). Rabbit polyclonal antibody against HMGB1 was provided by Shino-Test Corporation (Kanagawa, Japan). Antibodies against phospho- and total extracellular signal-regulated kinase (ERK)-1/2 were obtained from Cell Signaling Technology (Beverly, MA). U0126 was obtained from Calbiochem (La Jolla, CA).

Human Vitreous Samples

This study was approved by our institutional ethical committee (Kagoshima University Hospital), and was performed in accordance with the Declaration of Helsinki. All surgeries were performed at Kagoshima University Hospital. All patients gave informed consent before treatment. The clinical histories of all patients were obtained from their medical records. Undiluted vitreous fluid samples (0.5–0.7 ml) were obtained by pars plana vitrectomy. Vitreous humor was collected in sterile tubes, placed immediately on ice, centrifuged to remove cells and debris, and stored at −80°C until analysis.

Animals

All animal experiments were performed in accordance with the Association for Research in Vision and Ophthalmology Statement for the Use of Animals in Ophthalmic and Visual Research and the approval of our institutional animal care committee (Kagoshima University). Adult male Brown Norway rats (250–300 g; KBT Oriental, Saga, Japan) were housed in covered cages and kept at constant temperature and relative humidity with a regular 12-h light–dark schedule. Food and water were available *ad libitum*.

Surgical Induction of RD

Rat experimental RD was induced as described previously.[22] Briefly, the rats were anesthetized with an intramuscular injection of ketamine and xylazine, and their pupils were dilated with topical 1% tropicamide and 2.5% phenylephrine hydrochloride. The retinas were detached using a subretinal injection of 1% sodium hyaluronate (Opegan; Santen, Osaka, Japan) with an anterior chamber puncture to reduce intraocular pressure. Sodium hyaluronate (0.05 ml) was slowly injected through the sclera into the subretinal space to enlarge the RDs. These procedures were performed only in the right eye, with the left eye serving as a control. Eyes with lens injury, vitreous hemorrhage, infection, and spontaneous reattachment were excluded from the following analysis. The rats were killed at 3, 7, and 14 days after treatment, with six animals per each time point.

Cell Culture

The rat immortalized retinal precursor cell line R28, a kind gift from Dr GM Siegel (The State University of New York, Buffalo), was cultured in Dulbecco's modified Eagle's medium (DMEM) high glucose supplemented with 10% fetal bovine serum (FBS), 10 mM non-essential amino acids, and 10 μg/ml gentamicin as described previously.[23] The human immortalized RPE cell line ARPE-19, obtained from American Type Culture Collection (Manassas, VA), was grown in DMEM/F12 supplemented with 10% FBS, 2% penicillin–streptomycin, and 1% fungizone (all products were obtained from Invitrogen-Gibco, Rockville, MD). Cells were incubated at 37°C in a 5% CO_2 incubator and subcultured with 0.05% trypsin-EDTA. Subconfluent cultures were trypsinized and seeded for the following experiments. ARPE-19 cells were obtained at passage 21 and used at passages 24–30. Increased passage did not alter the following experimental results up to this passage number.

Cell Viability Assay

Cell viability was analyzed by mitochondrial respiratory activity measured using MTT (3-(4,5-dimethylthiazol-2yl)-2,5-diphenol tetrazolium bromide) assay (Wako Chemicals,

Osaka, Japan), as described previously.[24] Briefly, 2×10^5 R28 cells were cultured in 24-well plates (500 μl medium per well) with or without hydrogen peroxide (1 mM; Merck, Darmstadt, Germany) for 24 h. Then the cells were incubated with MTT (0.5 mg/ml; final concentration) for 3 h. Formazan product was solubilized by the addition of dimethyl sulfoxide for 16 h. Dehydrogenase activity was expressed as absorbance at a test wavelength of 570 nm and at a reference wavelength of 630 nm. Assays were performed in triplicate and repeated three times in independent experiments.

Immunofluorescence for HMGB1 and TUNEL

Indirect immunofluorescence was carried out as described previously,[19,25] with some modifications. The eyes were harvested and fixed in 4% paraformaldehyde at 4°C overnight. The anterior segment and the lens were removed, and the remaining eye cup was cryoprotected with 10–30% sucrose in phosphate-buffered saline. The eye cups were then frozen in an optimal cutting temperature compound (Sakura Finetech, Tokyo, Japan). Sections were cut at 8 μm with a cryostat (Leica Microsystems, Wetzler, Germany). After being incubated with blocking buffer containing 10% goat serum, 1% bovine serum albumin (BSA), and 0.05% Tween-20 for 1 h, the slides were incubated with rabbit polyclonal anti-HMGB1 antibody (1 μg/ml). After overnight incubation, sections were washed and probed with Alexa-Fluor 594-conjugated goat anti-rabbit IgG F(ab′)2 fragment (Molecular Probes, Carlsbad, CA) for 1 h. In some experiments, TUNEL co-staining was also performed according to the manufacturer's protocol (ApopTag Fluorescein *In situ* Apoptosis Detection kit; Chemicon, Temecula, CA) as previously described.[22] Slides were counterstained with DAPI, mounted with Shandon PermaFlour (Thermo Scientific, Waltham, MA), and viewed with a Zeiss fluorescence microscope. Images were captured using the same exposure time for each comparative section. To examine the specificity of immunostaining, the primary antibody was replaced with normal rabbit IgG (1 μg/ml). Control slides were invariably negative under the same setting (data not shown). For all experiments, at least three sections from each eye were evaluated. To demonstrate the expression patterns of HMGB1 in retinal cells under oxidative stress *in vitro*, R28 cells (2×10^5 cells/500 μl medium per well) were seeded on four-well glass coverslips and challenged with or without hydrogen peroxide (1 mM) for 1 h. Slides were fixed in 4% paraformaldehyde for 1 h, permeabilized with Triton X-100, and then examined by the same methods as described above.

ELISAs

HMGB1 and MCP-1 were quantified in each human vitreous sample using commercial ELISAs; HMGB1 ELISA kit (Shino-Test Corporation) and Human CCL2/MCP-1 Immunoassay (R&D Systems, Minneapolis, MN), according to the manufacturers' protocols. The detection limits of these kits were 0.2 ng/ml for HMGB1 and 5.0 pg/ml for MCP-1. Concentrations below the limits were taken as zero in subsequent analyses. Each sample was run in duplicate and compared with a standard curve. All samples were assessed in a masked manner. The mean concentration was determined per sample. For *in vitro* study, HMGB1 levels in culture supernatants were measured by the same ELISA.

Migration Assay

Cell migration was assayed using a modified Boyden chamber assay as previously described.[26] In brief, 5×10^4 ARPE-19 cells resuspended in 200 μl control medium (1% FBS-DMEM/F12) were seeded onto the upper compartment of the BD Falcon® culture inserts (BD Bioscience, San Jose, CA) with an 8-μm diameter pore size membrane in a 24-well companion plate. The lower chamber was filled with control medium (negative control) and those containing 50, 100, or 200 ng/ml rHMGB1. Because MCP-1 was reported to display a potent chemotactic activity on RPE cells,[27] a control medium containing 10 ng/ml rMCP-1 was used as a positive control. After 8-h incubation, cells remaining on the upper surface of the filters were removed mechanically, and those that had migrated to the lower surface were fixed with methanol, stained with Diff-Quick (Dade-Behring, Deerfield, IL), and counted in five randomly selected high-power fields ($\times$ 100) per insert. Migration index (% of control) was calculated by dividing the number of migrating cells in the presence of chemoattractants by the cells that migrated in response to the negative control. To inhibit ERK-1/2 activity, the cells were pretreated with 1, 5, or 10 μM U0126, or vehicle (0.1% dimethyl sulfoxide) for 30 min, prior to the addition of rHMGB1. U0126 is an inhibitor of active and inactive MEK-1/2, the MAPK kinase that activates ERK-1/2. These concentrations of U0126 and dimethyl sulfoxide had no effect on ARPE-19 cell viability determined by MTT assay in our study (data not shown) and in a previous report.[28] Assays were performed in triplicate and repeated three times in independent experiments.

Immunoblotting

ARPE-19 cells (5×10^5) were subcultured on 6-cm tissue culture dishes. Then, the cells were serum starved overnight in DMEM/F12 and stimulated with 100 ng/ml rHMGB1 for the indicated times. Activation of ERK-1/2 was analyzed as described previously.[24] In brief, after treatment, whole cells were lysed with SDS sample buffer and an equal volume of protein extracts was loaded onto 12% SDS-polyacrylamide gels and then transferred onto a nitrocellulose membrane. The membrane was blocked by incubation with 5% non-fat dry milk plus 1% BSA in TBST (0.02% Tween-20 in Tris-buffered saline, pH 7.4) for 1 h at room temperature. The membrane was then incubated with the antibody against phospho-ERK-1/2 (diluted 1/1000) at 4°C overnight. The blots were subsequently probed with secondary anti-rabbit antibodies conjugated to horseradish peroxidase (diluted 1/3000 in TBST), and images were developed using the en-

hanced chemiluminescence system (GE Healthcare). The membrane was stripped and reprobed with an antibody against total ERK-1/2 (diluted 1/1000).

Statistical Analysis

The vitreous HMGB1 and MCP-1 concentrations in each group were compared using the Mann–Whitney *U*-test. The correlation between HMGB1 and MCP-1 in RD samples was analyzed using a simple linear regression analysis and Spearman's rank correlation coefficient. All *in vitro* data are presented as mean ± s.d. and the significance of differences between groups was determined by Student's *t*-test. *P*-value less than 0.05 was considered significant.

RESULTS

HMGB1 is Present in Cultured Retinal Cell and Released Extracellularly by Oxidative Stress-Induced Cell Death

We first evaluated the expression patterns and cellular distribution of HMGB1 in an R28 retinal cell line with or without oxidative stress, a known cause of neurodegeneration.[29] Excessive reactive oxygen species can lead to the destruction of cellular components and ultimately induce cell death through apoptosis or necrosis. To induce oxidative stress, we used a toxic dose (1 mM) of hydrogen peroxide, which was reported to stimulate monocytes/macrophages to release HMGB1 actively and passively.[30] As shown in Figure 1a, HMGB1 immunoreactivity was stably present in the nucleus of unstimulated R28 cells, and relatively weak staining was observed in the cytoplasm. By contrast, 1 h after exposure to 1 mM hydrogen peroxide, some cells seemed to present rather high levels of HMGB1 in their nucleus as well as their cytoplasm compared with those under an unstimulated condition. However, in the other cells, the nuclear HMGB1 was diminished or appeared to be released into the cytoplasm. These results indicate that the nuclear HMGB1 could be varied by death stress and be released into the cytoplasm according to the degree of stress. Hydrogen peroxide (1 mM) treatment for 24 h, in which about 90% of the cells lost their viability (Figure 1b), induced a massive release of HMGB1 from the cells to the cell supernatants (Figure 1c). Taken together, these findings suggested that HMGB1 could relocate from the nucleus to the cytoplasm for eventual release in dying retinal cells, and that the extracellular release of HMGB1 in the eye might be increased dependent on the extent of retinal cell death.

HMGB1 is Abundantly Expressed in Rat Retina and Released after RD

As the above findings indicated that HMGB1 was of relevance to retinal cell death, we investigated whether HMGB1 was maintained in the rat retina and how HMGB1 would vary after RD. As it was reported that HMGB1 in rat photoreceptors had a light-sensitive circadian rhythmic expression,[25] we performed all animal studies on a regular time schedule, and all eyes were set to be almost equally exposed to light. As shown in Figure 2, HMGB1 immunoreactivity was well represented in sections of the normal control rat retina and, as expected, colocalized with DAPI-positive nuclei (Figure 2a, d and g). HMGB1 staining in the normal rat retina was prominent in the nuclei of ganglion cell layer, inner nuclear layer, outer nuclear layer, and RPE, and was also apparent in the photoreceptor inner segments. In particular, HMGB1 was localized in photoreceptor at the nuclear periphery, and HMGB1 levels were higher in the inner nuclear layer than the outer nuclear layer as opposed to DAPI staining, which preferred to bind to heterochromatic DNA. This was consistent with the previous report[25] that HMGB1 was preferentially colocalized with euchromatin, which was often under active transcription and was stained less by DAPI. Interestingly, HMGB1 appeared to be robustly upregulated in both the photoreceptors and the other retinal cells at day 3 after RD inductions, and DAPI staining was inversely downregulated at the same time (Figure 2b, e and h). As previous reports demonstrated that dramatic alterations of retinal gene expression occurred after RD,[31] this high level of HMGB1 expression might be related to the active gene transcription. HMGB1 in the nucleus might be stress responsive and necessary for proper transcription after RD tissue damage. Afterwards, the nuclear HMGB1 expression in the photoreceptors seemed to subside at day 7, while still clearly remained in the inner segments (Figure 2c, f and i), gradually decreasing along with the thinning of the outer nuclear layer due to photoreceptor degeneration by day 14 (data not shown).

Although HMGB1 expression was increased in the photoreceptors of the detached retina at day 3, it was not homogeneous, but was rather heterogeneous. To clarify the relationship between the upregulation of HMGB1 and photoreceptor cell death, especially with DNA damage, the RD retina at day 3 was co-stained with TUNEL, which could detect apoptotic and potentially necrotic cell death by labeling the damaged DNA (Figure 3a–c). Previous studies indicated that HMGB1 could not be released from apoptotic cells[6] and the apoptotic photoreceptors were prominent in this RD model at day 3 after RD.[22] We also confirmed remarkable numbers of apoptotic photoreceptors in the detached retina at day 3 (Figure 3b), and found that the early faint TUNEL-positive nuclei had relatively low levels of HMGB1 and fragmented nuclei, which were brightly stained by TUNEL, had almost no apparent HMGB1 immunoreactivity (Figure 3c), suggesting that apoptotic dying cells might lose the expression of HMGB1 to maintain the proper gene transcription. It might be indispensable for the surviving photoreceptors to maintain and/or boost the nuclear HMGB1 in RD.

In the subretinal space of RD at day 7, HMGB1-positive and TUNEL-negative debris could be observed (Figure 3d, arrows), which might be released by necrotic photoreceptors and/or degradated inner segments, and spread diffusely into the vitreous cavity if a retinal break was present. It was also

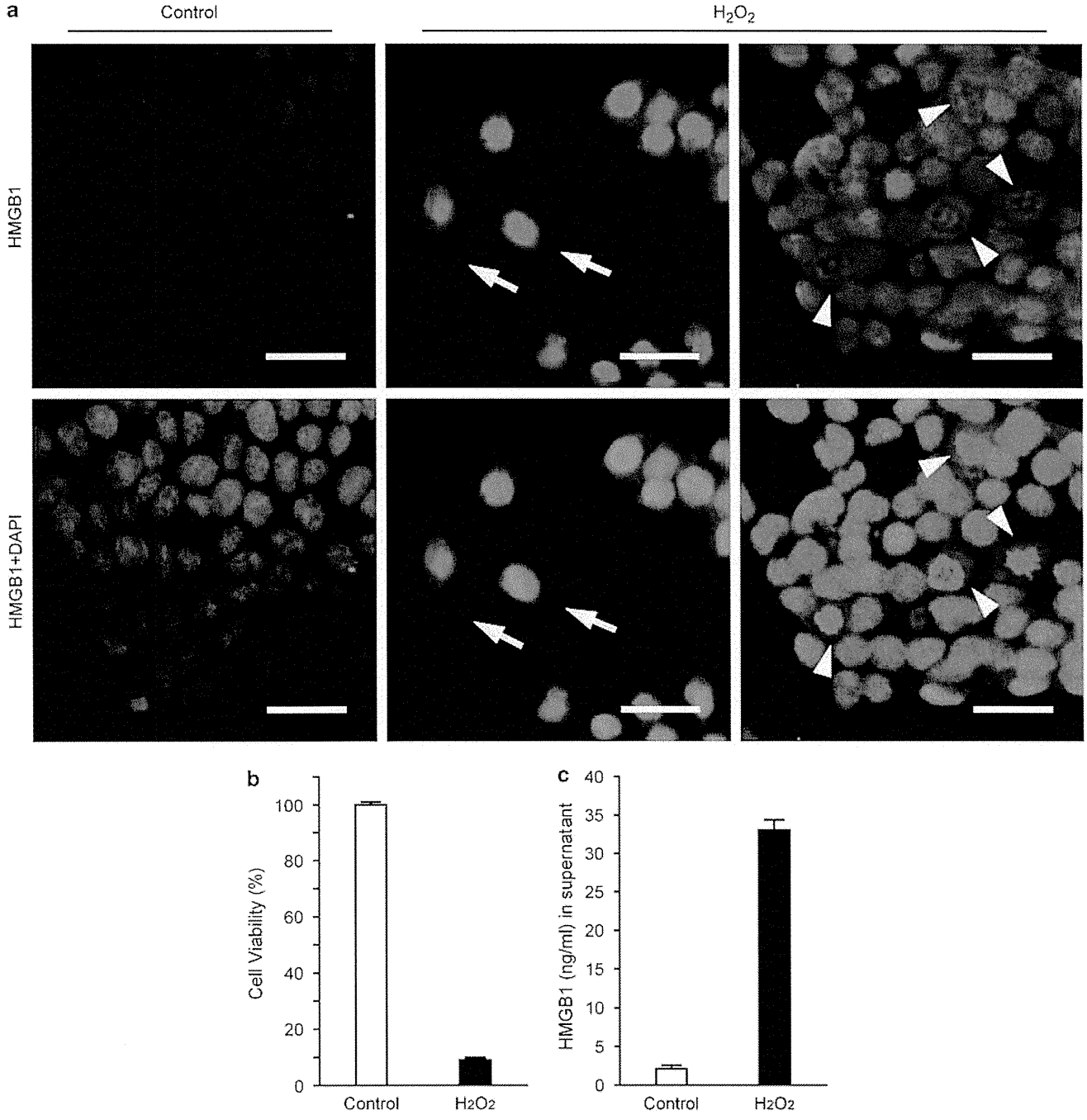

Figure 1 Release of HMGB1 from R28 retinal neuronal cells exposed to excessive oxidative stress. (**a**) Immunofluorescence was performed with anti-HMGB1 antibody (red) and DAPI (blue). HMGB1 is predominantly present in the nuclei of unstimulated R28 cells (left column). Some cells present robust upregulation of HMGB1 in the nuclei, as well as relocation into the cytoplasm (middle column; arrows) on 1 h exposure to a toxic dose of hydrogen peroxide (1 mM). In the other cells, the nuclear HMGB1 is found to be diminished or released into the cytoplasm (right column; arrowheads). Scale bars: 20 μm. (**b**) After 24 h exposure to 1 mM hydrogen peroxide, the cell viability analyzed by MTT assay is decreased to about 10% compared with the control. (**c**) Massive HMGB1 release into the culture supernatant was determined by ELISA after the same treatment as (**b**). The data represent the mean ± s.d. ($n = 3$). Similar results were obtained from three independent experiments.

Figure 2 Immunofluorescence analysis of HMGB1 in a rat model of RD. Representative photomicrographs of retinal sections labeled with anti-HMGB1 antibody (red; **a**–**c**) and DAPI (blue; **d**–**f**). Merged images (**g**–**i**) are also presented. The retinal sections were derived from the control eye (**a**, **d**, **g**), those at 3 days (day 3; **b**, **e**, **h**), or 7 days after RD (day 7; **c**, **f**, **i**). Arrows point to retinal pigment epithelium (**a**, **g**), and arrowheads indicate subretinal macrophages (**b**, **c**, **h**, **i**). Note that expression of HMGB1 is augmented especially in ONL at day 3 after RD, whereas the upregulation in ONL appears to be subside by day 7 ($n = 6$ for each time point). Scale bars: 50 μm. INL, inner nuclear layer; IS, inner segment; ONL, outer nuclear layer.

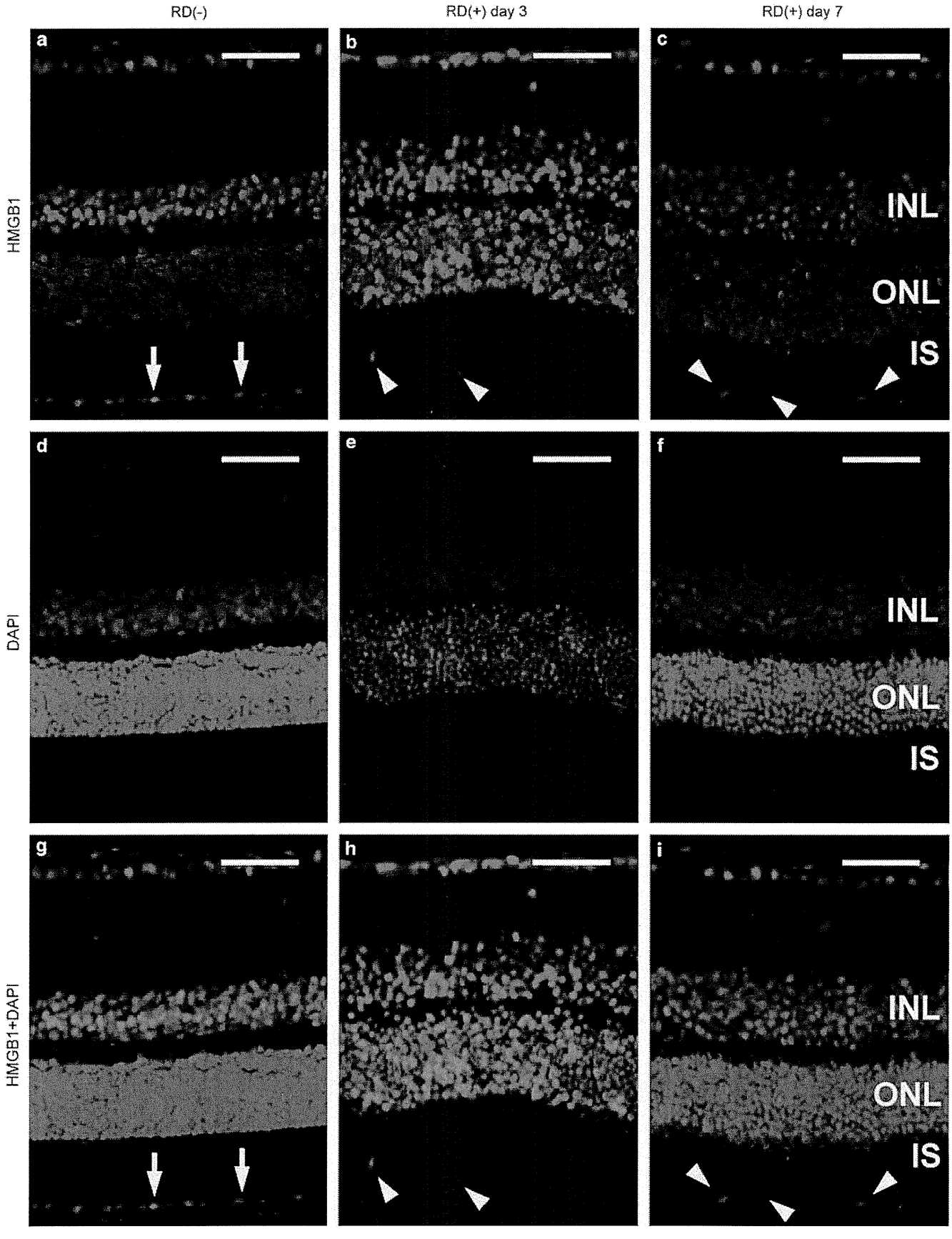
RD(-)
RD(+) day 3
RD(+) day 7
HMGB1
DAPI
HMGB1+DAPI
a
b
c
d
e
f
g
h
i
INL
ONL
IS
INL
ONL
IS
INL
ONL
IS

reported that macrophages migrated into the subretinal space of this RD model.[32] The migrating macrophages also had abundant HMGB1 expression (Figure 3d, arrowheads), and might have released HMGB1 actively in this space. In line with these data, a large amount of extracellular HMGB1 must be present at least in the subretinal space after RD.

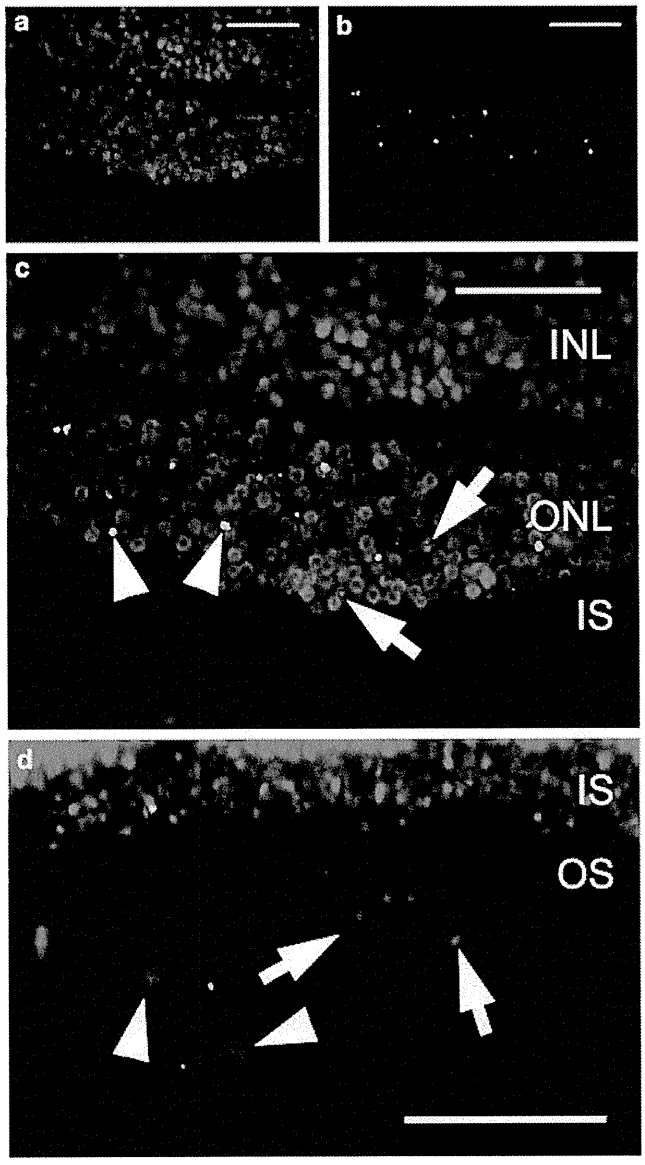

Figure 3 Expression of HMGB1 in DNA-damaged photoreceptors (**a**–**c**) and release of HMGB1 in the subretinal space (**d**). Representative photomicrographs of anti-HMGB1 antibody (red; **a**), TUNEL (green; **b**), and merged image (**c**) from rat retinal sections at 3 days after RD ($n=6$). The early faint TUNEL-positive nuclei (**c**; arrows) have relatively low levels of HMGB1 and the fragmented nuclei (**c**; arrowheads) have almost no apparent HMGB1 immunoreactivity. (**d**) Representative photomicrograph of a merged image of anti-HMGB1 (red), DAPI (blue), and TUNEL (green) obtained from rat retinal sections at 7 days after RD ($n=6$). HMGB1-positive and TUNEL-negative debris (**d**; arrows) and migrating macrophages with abundant HMGB1 expression (**d**; arrowheads) can be observed in the subretinal space. Scale bars: 50 μm. INL, inner nuclear layer; IS, inner segment; ONL, outer nuclear layer; OS, outer segment.

Vitreous HMGB1 and MCP-1 Levels in Patients with RD

The result obtained from the rat model of RD is the first evidence to our knowledge that HMGB1 is involved in RD-induced photoreceptor degeneration. Next, we tested whether extracellular HMGB1 could also be detected in human vitreous samples of RD. Samples were harvested from 35 eyes with RD, including rhegmatogenous RD, RD with macular hole, and atopic RD and 19 eyes with control diseases, including idiopathic epiretinal membrane and idiopathic macular hole (Table 1). The vitreous HMGB1 and MCP-1 levels were significantly higher in the eyes with RD than in those with control diseases (Figure 4). The median HMGB1 level was 1.4 ng/ml (range, 0–28.3) in the eyes with RD and 0.6 ng/ml (range, 0–1.3) in those with control diseases ($P<0.001$; Figure 4a). The median MCP-1 level was 1383.2 pg/ml (range, 39.8–5436.1) in the RD eyes and 404.4 pg/ml (range, 17.9–1168.9) in the control eyes ($P<0.0001$; Figure 4b). The vitreous concentration of HMGB1 was correlated significantly with that of MCP-1 in the 35 eyes with RD by a simple linear regression ($r=0.593$, $P<0.001$; Figure 4c) and by Spearman's rank correlation coefficient ($r=0.613$, $P<0.001$). On the other hand, there was no significant relationship between the vitreous concentrations of HMGB1 and MCP-1 in the 19 eyes of control patients (data not shown). Although there was no significant difference, the HMGB1 levels in the eyes with proliferative vitreoretinopathy (PVR), a condition of retinal fibrosis that follows severe long-standing RD, tended to be lower than those without PVR (Figure 4d). These findings showed that HMGB1 could be released not only in the subretinal space but also in the vitreous cavity after RD-induced photoreceptor degeneration, and that the HMGB1 release was coincident with vitreous MCP-1 expression.

Table 1 Characteristics of the patients

Characteristics	Retinal detachment ($n=35$)	Control diseases ($n=19$)
Age (years)	57.3 ± 16.3	68.2 ± 8.7
Female sex, no. (%)	19 (54)	10 (53)
Patients with PVR, no. (%)	6 (17)	—
Subgroups, no. (%)		
Rhegmatogenous retinal detachment	28 (80)	—
Retinal detachment with macular hole	5 (14)	—
Atopic retinal detachment	2 (6)	—
Idiopathic epiretinal membrane	—	7 (37)
Idiopathic macular hole	—	12 (63)

PVR, proliferative vitreoretinopathy.
Values are expressed as mean ± s.d. Dashes denote not applicable.

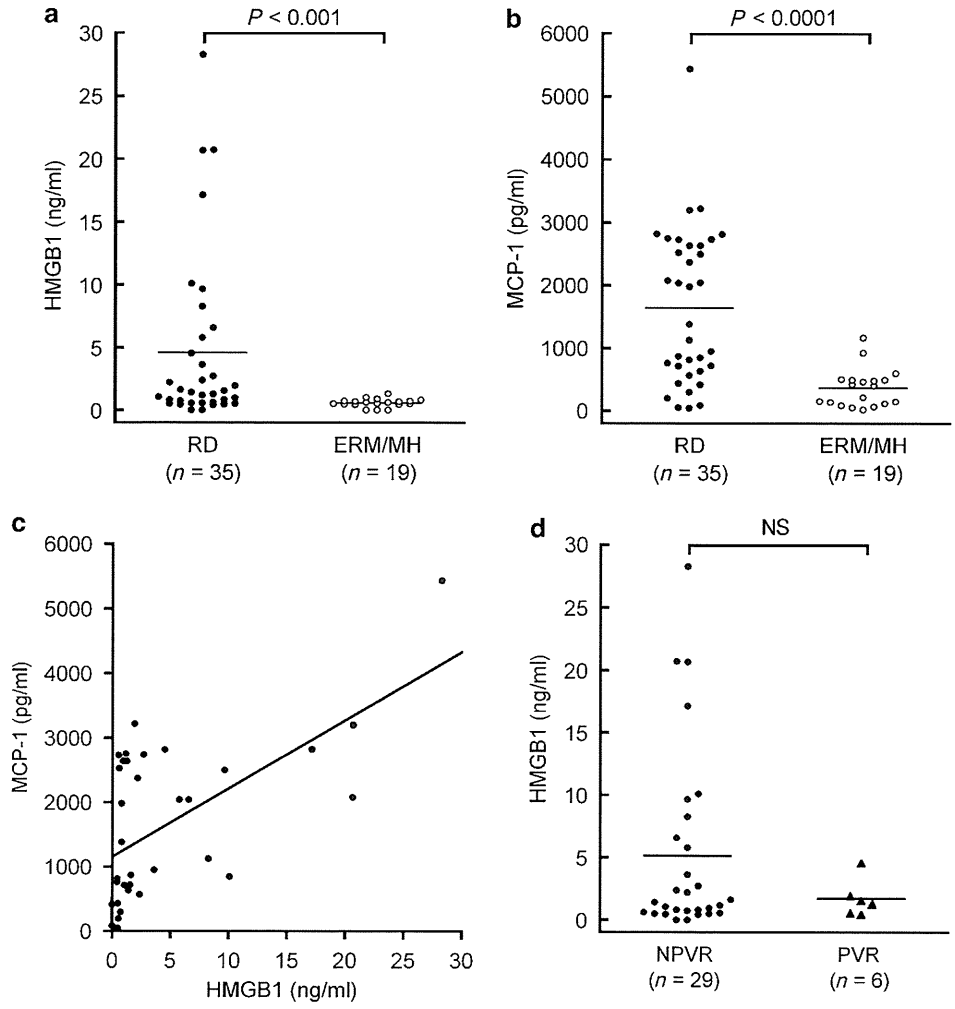

Figure 4 Vitreous levels of HMGB1 and MCP-1. The vitreous HMGB1 (**a**) and MCP-1 (**b**) levels are significantly higher in eyes with RD than in those with control diseases (idiopathic epiretinal membrane or idiopathic macular hole). Each bar indicates the average value. (**c**) Scatter plot for the correlation between vitreous levels of HMGB1 and MCP-1 in eyes with RD (simple linear regression, $r=0.593$, $P<0.001$; Spearman's rank correlation coefficient, $r=0.613$, $P<0.001$). (**d**) The HMGB1 levels in the eyes with PVR tend to be lower than those without PVR. ERM/MH, epiretinal membrane/macular hole; NPVR, no PVR; PVR, proliferative vitreoretinopathy.

RPE Cells Respond Chemotactically to Extracellular HMGB1 through an ERK-Dependent Mechanism

Previous reports have shown that extracellular HMGB1 is a chemoattractant for a variety of cell types.[21,33,34] We investigated whether HMGB1 is also a chemoattractant for RPE cells. Extracellular HMGB1 has been reported to engage multiple receptors, including the receptor for advanced glycation end products (RAGE) and Toll-like receptors 2 and 4.[2,4] In particular, RAGE has been thought to be a crucial receptor for HMGB1-induced cell migration through ERK activation.[33] The expression of RAGE at the RNA and protein level was identified in human RPE[35] and ARPE-19 cells[36,37] in previous studies. It was also shown that the expression of RAGE and HMGB1 was colocalized in the proliferative membrane from an eye with proliferative retinal disease.[38] We, therefore, performed a migration assay using modified Boyden chambers with various concentrations of rHMGB1. The representative photographs in Figure 5 show that rHMGB1 was capable of inducing a significant level of migration (Figure 5b) above that obtained with the control medium (Figure 5a). HMGB1 stimulated the migration of RPE cells in a concentration-dependent manner with a 2.7-fold maximal response at 100 ng/ml (Figure 5c). This maximal response to rHMGB1 was slightly stronger than that induced by rMCP-1 (10 ng/ml). Next, we investigated whether HMGB1 induced phosphorylation of ERK-1/2 in ARPE-19 cells; we stimulated cells with 100 ng/ml rHMGB1 for various time periods and used western blotting with an anti-phospho-ERK-1/2 antibody on whole-cell lysates (Figure 6a). Little phosphorylation of ERK-1/2 could be observed in unstimulated ARPE-19 (at 0 min), but a prominent increase was detected after 5 min of stimulation with rHMGB1. Figure 6a shows that phosphorylation of ERK-1/2 was augmented from 5 to 60 min after rHMGB1 stimulation in comparison

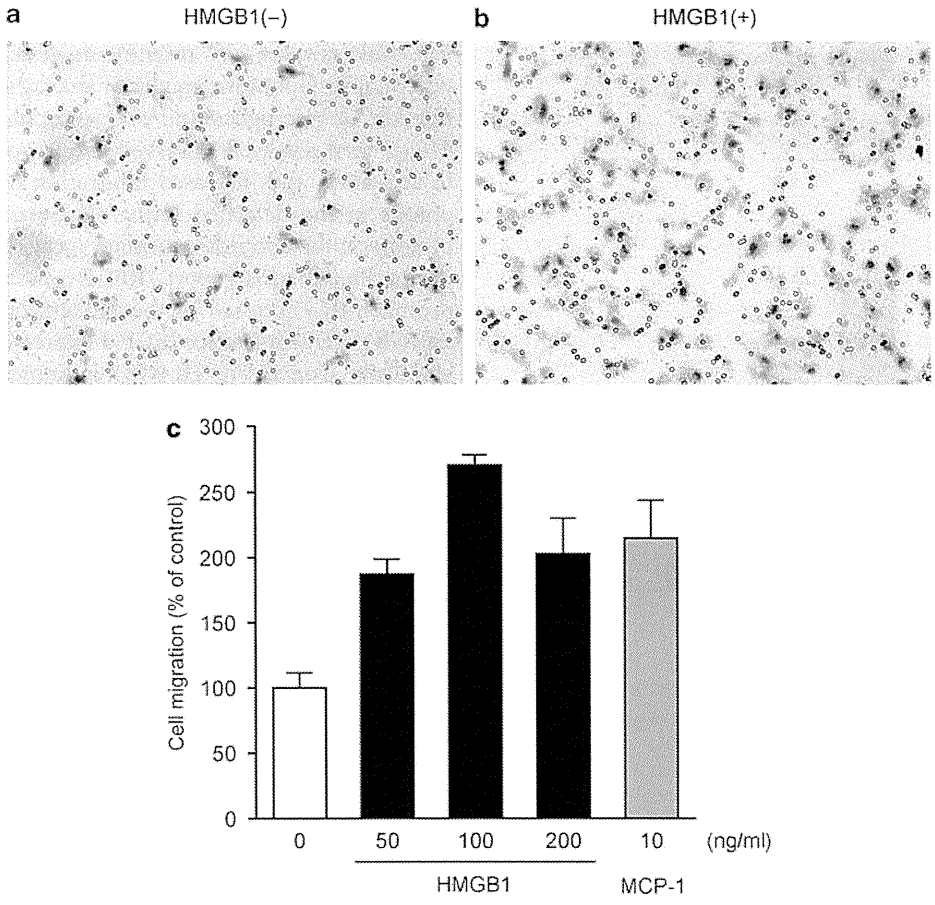

Figure 5 RPE cells migrate in response to HMGB1. Representative photographs of ARPE-19 cells stained with Diff-Quick after migration toward control medium (**a**) or 100 ng/ml HMGB1 (**b**). Original magnification: × 100. (**c**) HMGB1 stimulated ARPE-19 cell migration in a concentration-dependent manner with a 2.7-fold maximal response at 100 ng/ml. The data represent the mean ± s.d. ($n = 3$). All treatments increase the migratory response relative to the control ($P < 0.01$ in Student's *t*-test). Similar results were obtained from three independent experiments.

with unstimulated ARPE-19 (time 0). To demonstrate that the ERK signaling induced by HMGB1 was in fact linked to the migration of RPE cells, we next inhibited ERK-1/2 and assessed cell migration to HMGB1. Pretreatment of ARPE-19 with U0126 abrogated the migration toward rHMGB1 (Figure 6b). Thus, the ERK pathway appears to play an essential role in HMGB1-induced RPE cell migration.

DISCUSSION

Our findings suggest a possible role of HMGB1 in RD, as an essential nuclear protein and a principal danger signal for photoreceptor degeneration. Using an *in vitro* assay of retinal cell death induced by excessive oxidative stress, we found that HMGB1 was augmented in the nucleus by the stress and released into the extracellular space during cell death. On the basis of immunohistochemical analyses of a rat model of RD-induced photoreceptor degeneration, augmentation of HMGB1 in the nucleus is also observed *in vivo* and appears to be crucial for the proper transcription of photoreceptors after RD. Moreover, double labeling with TUNEL reveals defects of upregulation of the nuclear HMGB1 in the DNA-damaged photoreceptors, which are presumably programmed dying photoreceptors. Therefore, we propose that the nuclear HMGB1 in the retinal cells might be critical for retinal cell survival under death stresses both in the *in vivo* RD and *in vitro* retinal cell death. These results for ocular HMGB1 are compatible with previous reports that HMGB1 is a vital nuclear protein and has a protective role in the nucleus.[2,4]

In a previous animal study, Erickson *et al*[17] reported that a loss of photoreceptors in a cat model of RD occurred due to necrosis. During studies on RD, photoreceptor degeneration after RD had been thought to be mainly caused by apoptosis.[15,16] Hisatomi *et al*[32] demonstrated the presence of apoptotic debris in the subretinal space of rat RD. In the present study, considering our immunohistochemistry results from the same rat model of RD, so-called necrotic debris, which is HMGB1 positive and TUNEL negative, was found to be present. On the basis of the previous finding of the preferential release of HMGB1 from necrotic cells,[6] this suggests that necrosis might still be a fundamental type of photoreceptor cell death after RD.

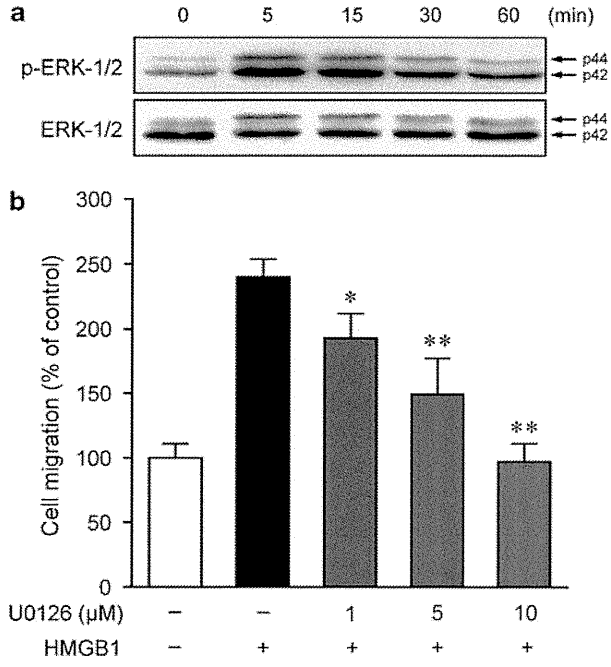

Figure 6 The phosphorylation of ERK is induced by HMGB1 and linked to HMGB1-induced migration of RPE cells. (**a**) ARPE-19 cells were stimulated with HMGB1 (100 ng/ml) for 5, 15, 30, or 60 min, and total cell lysates were analyzed by western blot. ERK-1/2 activation was detected with anti-phospho-ERK-1/2 antibody (p-ERK-1/2). Stripped membrane was reprobed with the antibody against total ERK-1/2 (ERK-1/2). Results are representative of three independent experiments. HMGB1 augments the ERK-1/2 phosphorylation from 5 to 60 min after stimulation. (**b**) Pretreatment of ARPE-19 with U0126 inhibits the cell migration toward HMGB1 (100 ng/ml) in a dose-dependent manner. The data represent the mean ± s.d. ($n = 3$). Similar results were obtained from three independent experiments. $^{*}P < 0.05$, $^{**}P < 0.01$, compared with vehicle-treated control.

Furthermore, exploring human vitreous samples by ELISA, we found that both HMGB1 and MCP-1 are increased significantly in eyes with RD. Although MCP-1 is a well-known mediator for RD,[39] to our knowledge, this is the first report indicating that extracellular HMGB1 might also be of relevance to human RD. HMGB1 concentration tended to be high in the eye without PVR, but not so with PVR. One possible explanation for this tendency is that HMGB1 might be sequestered and/or masked in PVR, the advanced stage of RD. HMGB1 binds tightly to heparin and proteoglycans with heparan sulfate,[5] and it is also reported that such proteoglycans are abundantly present as the ocular extracellular matrix, even in RD.[40] Hence, these molecules might affect the HMGB1 concentration in the vitreous humor. Nevertheless, this possibility does not negate the presence of HMGB1. Considering the results obtained with the rat RD model, extracellular HMGB1 could be present at much higher levels, at least in the subretinal fluid of RD, and it might serve as a persistent signal adhering to the local damaged retina and/or surrounding matrix as previously described.[5]

It is also of importance that HMGB1 is significantly correlated with MCP-1 in RD vitreous. The secretion of MCP-1 might parallel the extent of photoreceptor degeneration of RD. Nakazawa *et al*[20] recently suggested that MCP-1 is a potential proapoptotic mediator during RD through the activation of microglias and/or macrophages. In their study, Müller-glial cells were observed to upregulate MCP-1, leading to activation and increased infiltration of microglias/macrophages in the detached retina. These cells induced further photoreceptor apoptosis through local oxidative stress. Corresponding to this report, RAGE was also reported to be prominently expressed in the Müller-glial cells.[41] Therefore, HMGB1 might influence MCP-1 expression through Müller-glial cells. Conversely, HMGB1 is known to be released by activated monocytes/macrophages.[7] MCP-1 is a potent stimulator and chemoattractant for monocytes/macrophages,[42] and these cells were observed in the subretinal space of RD with abundant HMGB1 expression. This would also be another possible explanation for the parallel increases of HMGB1 and MCP-1. Nevertheless, the positive correlation of these molecules indicates that cell death-related mediators might be highly orchestrated in ocular degenerative tissue damage. Several studies suggest that extracellular HMGB1 can aggravate tissue damage in neuronal tissues.[10,43] In these studies, extracellular HMGB1 plays a key role in the development of neuronal injury through the induction of inflammation, microglial activation, and neuronal excitotoxicity. According to these recent reports, the presence of extracellular HMGB1 concomitantly with MCP-1 is a possible deteriorating factor for RD, in spite of its essential role in the nucleus.

PVR is one of the most threatening complications of RD. It is thought to be a reactive process to retinal injury, in other words, it is one of the wound-healing responses in the eye. RPE cells are known to be detectable in the fibrotic proliferative membranes of PVR, and play an important role in the pathogenesis of PVR.[44] Thus, the effects of a molecule on PVR formation could be traced to RPE migration, at least in part. Here, we demonstrate that extracellular HMGB1 promotes RPE cell migration by chemotaxis *in vitro*. This result is consistent with previous reports of HMGB1-induced cell migration in various cell types, such as smooth muscle cells,[21,33] fibroblasts,[45] and chondrocytes.[34] We also found that HMGB1 activated phosphorylation of ERK-1/2 in RPE cells and the migration induced by HMGB1 was dependent on ERK phosphorylation. The phosphorylation of ERK is associated with cell proliferation and cell migration through effects on cell–matrix contacts.[46] It was also reported to be found in Müller-glial cells after RD.[47] Taken together, our results suggest that extracellular HMGB1 from dying ocular cells might affect retinal cells through ERK phosphorylation and potentially serve to promote the formation of PVR, which is wound healing, but has a pathological meaning in the eye. Several new strategies for prevention of ocular fibrosis, especially targeting specific signaling pathways, have been proven to be beneficial in animal models.[48–50] We propose that the identification and further characterization of danger signals, including HMGB1, would provide a novel

perspective for better understanding the molecular pathogenesis of PVR before applying these promising therapeutic manipulations to human subjects.

It has been suggested that post-transcriptional modifications of HMGB1, such as acetylation, methylation, and phosphorylation, might influence its activity.[51] Some recent reports also demonstrate that the proinflammatory activity of HMGB1 is due to combined action with other molecules.[52] The present data are mostly limited to the presence of HMGB1 rather than its biological activity, and we do not address what modifications or molecules are involved in intraocular HMGB1. However, we identify for the first time that HMGB1 is evident in a typical retinal injury of human RD, in which nuclear HMGB1 is a crucial nuclear protein and extracellular HMGB1 is a danger signal that might be required for the ocular wound-healing response. Our findings might have relevance for the underlying mechanisms of degenerative neuronal diseases. Further detailed studies will be needed to obtain more accurate knowledge and therapeutic value of HMGB1 in human diseases.

ACKNOWLEDGEMENTS

We thank Dr GM Siegel, The State University of New York, for providing R28 cells; Drs Takashi Ito, Yoko Oyama, Toshiaki Shimizu, Kazunori Takenouchi, Kiyoshi Kikuchi, Masahiro Iwata, Yuko Nawa, Yoko Morimoto, Naoki Miura, and Noboru Taniguchi for their helpful advice and technical support; Miss Nobue Uto, Tomoka Nagasato, Hisayo Sameshima, and Maiko Yamaguchi for their assistance with the experiments. This research was supported in part by a grant from the Research Committee on Chorioretinal Degeneration and Optic Atrophy, Ministry of Health, Labor, and Welfare and by a grant-in-aid for Scientific Research from the Ministry of Education, Science, and Culture of the Japanese Government.

1. Bianchi ME. DAMPs, PAMPs and alarmins: all we need to know about danger. J Leukoc Biol 2007;81:1–5.
2. Ulloa L, Messmer D. High-mobility group box 1 (HMGB1) protein: friend and foe. Cytokine Growth Factor Rev 2006;17:189–201.
3. Martin P. Wound healing—aiming for perfect skin regeneration. Science 1997;276:75–81.
4. Lotze MT, Tracey KJ. High-mobility group box 1 protein (HMGB1): nuclear weapon in the immune arsenal. Nat Rev Immunol 2005;5:331–342.
5. Huttunen HJ, Rauvala H. Amphoterin as an extracellular regulator of cell motility: from discovery to disease. J Intern Med 2004;255:351–366.
6. Scaffidi P, Misteli T, Bianchi ME. Release of chromatin protein HMGB1 by necrotic cells triggers inflammation. Nature 2002;418:191–195.
7. Wang H, Bloom O, Zhang M, *et al.* HMG-1 as a late mediator of endotoxin lethality in mice. Science 1999;285:248–251.
8. Passalacqua M, Patrone M, Picotti GB, *et al.* Stimulated astrocytes release high-mobility group 1 protein, an inducer of LAN-5 neuroblastoma cell differentiation. Neuroscience 1998;82:1021–1028.
9. Ito T, Kawahara K, Nakamura T, *et al.* High-mobility group box 1 protein promotes development of microvascular thrombosis in rats. J Thromb Haemost 2007;5:109–116.
10. Kim JB, Sig Choi J, Yu YM, *et al.* HMGB1, a novel cytokine-like mediator linking acute neuronal death and delayed neuroinflammation in the postischemic brain. J Neurosci 2006;26:6413–6421.
11. Campana L, Bosurgi L, Rovere-Querini P. HMGB1: a two-headed signal regulating tumor progression and immunity. Curr Opin Immunol 2008;20:518–523.
12. Inoue K, Kawahara K, Biswas KK, *et al.* HMGB1 expression by activated vascular smooth muscle cells in advanced human atherosclerosis plaques. Cardiovasc Pathol 2007;16:136–143.
13. Taniguchi N, Kawahara K, Yone K, *et al.* High mobility group box chromosomal protein 1 plays a role in the pathogenesis of rheumatoid arthritis as a novel cytokine. Arthritis Rheum 2003;48:971–981.
14. Morimoto Y, Kawahara KI, Tancharoen S, *et al.* Tumor necrosis factor-alpha stimulates gingival epithelial cells to release high mobility-group box 1. J Periodontal Res 2008;43:76–83.
15. Cook B, Lewis GP, Fisher SK, *et al.* Apoptotic photoreceptor degeneration in experimental retinal detachment. Invest Ophthalmol Vis Sci 1995;36:990–996.
16. Arroyo JG, Yang L, Bula D, *et al.* Photoreceptor apoptosis in human retinal detachment. Am J Ophthalmol 2005;139:605–610.
17. Erickson PA, Fisher SK, Anderson DH, *et al.* Retinal detachment in the cat: the outer nuclear and outer plexiform layers. Invest Ophthalmol Vis Sci 1983;24:927–942.
18. Vazquez-Chona F, Song BK, Geisert Jr EE. Temporal changes in gene expression after injury in the rat retina. Invest Ophthalmol Vis Sci 2004;45:2737–2746.
19. Arimura N, Ki IY, Hashiguchi T, *et al.* High-mobility group box 1 protein in endophthalmitis. Graefes Arch Clin Exp Ophthalmol 2008;246:1053–1058.
20. Nakazawa T, Hisatomi T, Nakazawa C, *et al.* Monocyte chemoattractant protein 1 mediates retinal detachment-induced photoreceptor apoptosis. Proc Natl Acad Sci USA 2007;104:2425–2430.
21. Porto A, Palumbo R, Pieroni M, *et al.* Smooth muscle cells in human atherosclerotic plaques secrete and proliferate in response to high mobility group box 1 protein. FASEB J 2006;20:2565–2566.
22. Hisatomi T, Sakamoto T, Murata T, *et al.* Relocalization of apoptosis-inducing factor in photoreceptor apoptosis induced by retinal detachment *in vivo*. Am J Pathol 2001;158:1271–1278.
23. Neekhra A, Luthra S, Chwa M, *et al.* Caspase-8, -12, and -3 activation by 7-ketocholesterol in retinal neurosensory cells. Invest Ophthalmol Vis Sci 2007;48:1362–1367.
24. Biswas KK, Sarker KP, Abeyama K, *et al.* Membrane cholesterol but not putative receptors mediates anandamide-induced hepatocyte apoptosis. Hepatology 2003;38:1167–1177.
25. Hoppe G, Rayborn ME, Sears JE. Diurnal rhythm of the chromatin protein Hmgb1 in rat photoreceptors is under circadian regulation. J Comp Neurol 2007;501:219–230.
26. Hinton DR, He S, Graf K, *et al.* Mitogen-activated protein kinase activation mediates PDGF-directed migration of RPE cells. Exp Cell Res 1998;239:11–15.
27. Han QH, Hui YN, Du HJ, *et al.* Migration of retinal pigment epithelial cells *in vitro* modulated by monocyte chemotactic protein-1: enhancement and inhibition. Graefes Arch Clin Exp Ophthalmol 2001;239:531–538.
28. Glotin AL, Calipel A, Brossas JY, *et al.* Sustained versus transient ERK1/2 signaling underlies the anti- and proapoptotic effects of oxidative stress in human RPE cells. Invest Ophthalmol Vis Sci 2006;47:4614–4623.
29. Klein JA, Ackerman SL. Oxidative stress, cell cycle, and neurodegeneration. J Clin Invest 2003;111:785–793.
30. Tang D, Shi Y, Kang R, *et al.* Hydrogen peroxide stimulates macrophages and monocytes to actively release HMGB1. J Leukoc Biol 2007;81:741–747.
31. Hollborn M, Francke M, Iandiev I, *et al.* Early activation of inflammation- and immune response-related genes after experimental detachment of the porcine retina. Invest Ophthalmol Vis Sci 2008;49:1262–1273.
32. Hisatomi T, Sakamoto T, Sonoda KH, *et al.* Clearance of apoptotic photoreceptors: elimination of apoptotic debris into the subretinal space and macrophage-mediated phagocytosis via phosphatidylserine receptor and integrin alphavbeta3. Am J Pathol 2003;162:1869–1879.
33. Degryse B, Bonaldi T, Scaffidi P, *et al.* The high mobility group (HMG) boxes of the nuclear protein HMG1 induce chemotaxis and cytoskeleton reorganization in rat smooth muscle cells. J Cell Biol 2001;152:1197–1206.
34. Taniguchi N, Yoshida K, Ito T, *et al.* Stage-specific secretion of HMGB1 in cartilage regulates endochondral ossification. Mol Cell Biol 2007;27:5650–5663.
35. Yamada Y, Ishibashi K, Ishibashi K, *et al.* The expression of advanced glycation endproduct receptors in rpe cells associated with basal deposits in human maculas. Exp Eye Res 2006;82:840–848.

36. Howes KA, Liu Y, Dunaief JL, *et al.* Receptor for advanced glycation end products and age-related macular degeneration. Invest Ophthalmol Vis Sci 2004;45:3713–3720.
37. Ma W, Lee SE, Guo J, *et al.* RAGE ligand upregulation of VEGF secretion in ARPE-19 cells. Invest Ophthalmol Vis Sci 2007;48: 1355–1361.
38. Pachydaki SI, Tari SR, Lee SE, *et al.* Upregulation of RAGE and its ligands in proliferative retinal disease. Exp Eye Res 2006;82: 807–815.
39. Elner SG, Elner VM, Jaffe GJ, *et al.* Cytokines in proliferative diabetic retinopathy and proliferative vitreoretinopathy. Curr Eye Res 1995;14:1045–1053.
40. Wang JB, Tian CW, Guo CM, *et al.* Increased levels of soluble syndecan-1 in the subretinal fluid and the vitreous of eyes with rhegmatogenous retinal detachment. Curr Eye Res 2008;33:101–107.
41. Barile GR, Pachydaki SI, Tari SR, *et al.* The RAGE axis in early diabetic retinopathy. Invest Ophthalmol Vis Sci 2005;46: 2916–2924.
42. Matsushima K, Larsen CG, DuBois GC, *et al.* Purification and characterization of a novel monocyte chemotactic and activating factor produced by a human myelomonocytic cell line. J Exp Med 1989;169:1485–1490.
43. Pedrazzi M, Raiteri L, Bonanno G, *et al.* Stimulation of excitatory amino acid release from adult mouse brain glia subcellular particles by high mobility group box 1 protein. J Neurochem 2006;99:827–838.
44. Pastor JC, de la Rua ER, Martin F. Proliferative vitreoretinopathy: risk factors and pathobiology. Prog Retin Eye Res 2002;21:127–144.
45. Straino S, Di Carlo A, Mangoni A, *et al.* High-mobility group box 1 protein in human and murine skin: involvement in wound healing. J Invest Dermatol 2008;128:1545–1553.
46. Lawrence MC, Jivan A, Shao C, *et al.* The roles of MAPKs in disease. Cell Res 2008;18:436–442.
47. Nakazawa T, Takeda M, Lewis GP, *et al.* Attenuated glial reactions and photoreceptor degeneration after retinal detachment in mice deficient in glial fibrillary acidic protein and vimentin. Invest Ophthalmol Vis Sci 2007;48:2760–2768.
48. Saika S. TGFbeta pathobiology in the eye. Lab Invest 2006;86 :106–115.
49. Saika S, Yamanaka O, Nishikawa-Ishida I, *et al.* Effect of Smad7 gene overexpression on transforming growth factor beta-induced retinal pigment fibrosis in a proliferative vitreoretinopathy mouse model. Arch Ophthalmol 2007;125:647–654.
50. Saika S, Yamanaka O, Sumioka T, *et al.* Fibrotic disorders in the eye: targets of gene therapy. Prog Retin Eye Res 2008;27:177–196.
51. Bianchi ME, Manfredi AA. High-mobility group box 1 (HMGB1) protein at the crossroads between innate and adaptive immunity. Immunol Rev 2007;220:35–46.
52. Sha Y, Zmijewski J, Xu Z, *et al.* HMGB1 develops enhanced proinflammatory activity by binding to cytokines. J Immunol 2008;180:2531–2537.

Ultrasound in Med. & Biol., Vol. 35, No. 11, pp. 1845–1853, 2009

0301-5629/09/$–see front matter

ELSEVIER

doi:10.1016/j.ultrasmedbio.2009.05.023

● *Original Contribution*

SONOTHROMBOLYSIS FOR INTRAOCULAR FIBRIN FORMATION IN AN ANIMAL MODEL

TOSHIFUMI YAMASHITA,* HIROKI OHTSUKA,* NOBORU ARIMURA,* SHOZO SONODA,* CHIHIRO KATO,† KANEO USHIMARU,† NAOKO HARA,† KATSURO TACHIBANA,‡ and TAIJI SAKAMOTO*

*Department of Ophthalmology, Kagoshima University Graduate School of Medical and Dental Sciences, Sakuragaoka, Kagoshima, Japan; †Tomey Corporation, Nagoya, Aichi, Japan; and ‡Department of Anatomy, Faculty of Medicine, Fukuoka University, Fukuoka, Japan

(*Received* 17 *October* 2008, *revised* 22 *May* 2009, *in final form* 28 *May* 2009)

Abstract—Vascular diseases such as diabetic retinopathy or retinal arterial occlusion are always associated with retinal and/or choroidal vasculopathy and intravascular thrombosis is commonly found. The ultrasound (US) therapy is a recently developed technique to accelerate fibrinolysis and it is being applied to some clinical fields. The present study was to observe the effects of extraocular US exposure on intraocular fibrin, which is a deteriorating factor in various ocular diseases. Tubes containing human blood (2 mL) in the following groups were irradiated with US; US alone, US with tissue plasminogen activator (tPA), tPA alone, and saline (control). Fibrinolysis was quantified by measuring D-dimer after 2 h. In rat eyes, intracameral fibrin (fibrin formation in the anterior chamber of the eye) was induced by YAG-laser-induced iris bleeding. Then, eyes in the following groups were irradiated with US; US alone, subconjunctival tPA alone, US and subconjunctival tPA, control. Intracameral fibrin was scored on day 3 (3+ maximum to 0). The temperatures of rat eyes were measured by infrared thermography. Histologic evaluation was also performed. D-dimer was increased by US with statistical significance ($p < 0.05$) or tPA ($p < 0.01$). D-dimer in US with tPA group was significantly higher than either US alone or tPA alone group ($p < 0.01$). In rat eyes, the average intracameral fibrin score on day 3 was 1.4 in control group and 1.2 in subconjunctival tPA alone group; however, it decreased significantly in the US alone group (0.75; $p < 0.05$, vs. control), US and subconjunctival tPA group (0.71; $p < 0.01$, vs. control). The temperature was less than 34 °C after US exposure. No histologic damage was observed. US irradiation from outside accelerated intracameral fibrinolysis without causing apparent tissue damage. This noninvasive method might have therapeutic value for intraocular fibrin. (E-mail: tsakamot@m3.kufm.kagoshima-u.ac.jp) © **2009 World Federation for Ultrasound in Medicine & Biology.**

Key Words: **Ultrasound, Fibrinolysis, Thrombolysis, Sonothrombolysis, Tissue plasminogen activator.**

INTRODUCTION

Vascular diseases such as diabetic retinopathy are the leading causes of legal blindness in adults in western societies. These diseases are always associated with retinal and/or choroidal vasculopathy and intravascular thrombosis is commonly found to some extent (Vine and Samama 1993). Among them, retinal arterial occlusion (RAO) has a poor prognosis (Hayreh 2008). Furthermore, fibrin formation in the vitreous and/or anterior chamber is sometimes observed after intraocular surgery, leading to secondary tissue damage (Akassoglou et al. 2004; Jaffe et al. 1990; McDonald et al. 1990; Toth et al. 1991). To remove thrombus or fibrin, a fibrinolytic agent such as tissue-plasminogen activator (tPA) is sometimes used (Feltgen et al. 2006; Hayreh 2008; Kattah et al. 2002; Noble et al. 2008; Richard et al. 1999; Weber et al. 1998). However, the effect of fibrinolytic agents on these diseases is controversial and the potential toxicity of high doses of tPA cannot be neglected (Yamamoto et al. 2008; Yoeruek et al. 2008). Surgical removal of intravascular thrombus is another approach but its therapeutic value is also controversial (García-Arumí et al. 2006; Opremcak et al. 2008). Above all, the invasiveness and the potential risks of surgical embolus removal would make it difficult for physicians to accept these treatments.

The use of ultrasound (US) to accelerate fibrinolysis for thrombolytic therapy is a developed technique. It was

Address correspondence to: Taiji Sakamoto, Department of Ophthalmology, Kagoshima University Graduate School of Medical and Dental Sciences, Sakuragaoka, Kagoshima, Kagoshima 890-8520, Japan. E-mail: tsakamot@m3.kufm.kagoshima-u.ac.jp

evaluated by previous studies and has been found to have effects but less invasive potential for fibrinolysis (Francis et al. 1992; Holland et al. 2008; Hong et al. 1990; Lauer et al. 1992; Tachibana 1992; Tachibana K and Tachibana S 1995, 1997; Trübestein et al. 1976). Therefore, it is being applied in some clinical fields including peripheral vascular occlusions, acute myocardial infarctions (Cohen et al. 2003), occluded arteriovenous dialysis grafts (Pfaffenberger et al. 2005) and acute ischemic stroke. Early investigators showed that transcranial US increases fibrinolytic activity (Francis et al. 1995). Although a translational study using large US probes was hampered by an increased rate of intracerebral hemorrhage, phase-II Combined Lysis of Thrombus in Brain Ischemia Using Transcranial Ultrasound and Systemic t-PA trial that randomly assigned 126 patients with middle cerebral artery occlusion showed favorable results (Alexandrov et al. 2004; Daffertshofer et al. 2005).

In comparison to intracranial or visceral lesions, intraocular lesion is expected to be suitable for this treatment because responses to the treatment can be monitored in detail by direct observation and the therapeutic efficacy might be achievable with less power. So far, to the best of our knowledge, there have been no reports on sonothrombolytic treatment for ocular fibrin formation. In this study, we report on this new promising treatment approach for intracameral fibrin (fibrin formation in the anterior chamber of the eye) and evaluate its effects.

MATERIALS AND METHODS

In vitro study

Fibrin clot preparation. Venous blood was withdrawn from four healthy volunteers after they provided informed consent. Whole blood (2 mL) was immediately placed in disposable culture tubes. The tubes containing the blood were then placed in a 37°C water bath for 2 h referring to the previously described method (Frenkel et al. 2006).

US treatment. US was irradiated using a commercially available machine (Sonitron 2000; Richmar, Inola, OK, USA) with a 6 mm unfocused probe directly to the blood in the tubes (Borex, 12 × 75 mm disposable culture tubes, composed of borosilicate glass) in a tank of water at 37°C for various time intervals. Based upon our preliminary experiment, the parameters of US were determined as follows: frequency of 1.0 MHz, duty cycle of 5.2%, pulse repetition frequency of 20 Hz and the derated spatial-peak pulse-average intensity ($I_{SPPA.3}$) of 10.123 W/cm^2. First, US was irradiated with different exposure times, 5 min or 20 min (n=8, each). In addition, the temperature in the tube was measured after US irradiation for 20 min under the same condition (n = 4). Next, the experimental groups were divided into the following: US exposure alone (US, n = 8), US exposure with tPA (US + tPA, n = 8), tPA alone (tPA, n = 8) and saline alone (no US, no tPA, control, n = 8). tPA (Cleactor; Eisai, Tokyo, Japan) was diluted with saline (40 IU/μL) just before the experiment. Before the clots were exposed to US, tPA and saline (total 500 μL) were added to the tubes and incubated in a 37°C water bath for 2 h.

D-dimer assays. Because D-dimer is an indicator of fibrin-degraded products, a commercial D-dimer assay kit (Diagnostica Stago, Parsippany, NJ, USA) was used to measure D-dimer levels 2 h after treatment. The assays were performed according to directions provided by the manufacturer.

In vivo study

Safety of US exposure. Before application of US with animals, the output level of US was evaluated. We examined the safety of Sonitron 2000 with a 3 and 6 mm unfocused probes in consideration of application to human eyes. In brief, we measured acoustic power using a needle hydrophone in a water tank and assessed and computed some acoustic parameters (Schema 1). US was irradiated under the following conditions: frequency of 1.0 MHz, high or low intensity mode indicated on the device and duty cycle of 5.2% or 100%. Safety conditions referred to information of manufacturers seeking marketing clearance for diagnostic ultrasound systems and transducers by the Food and Drug Administration of the United States Department of Health and Human Services (FDA) (http://www.fda.gov/cdrh/ode/guidance/560.html#2).

Animals. All animals were used humanely in accordance with the approval of our institutional animal care committee and the ARVO statement on the Use of Animals in Ophthalmic and Vision Research. Brown-Norway rats (male; age 8-weeks old, 250 g) were purchased from KBT Oriental Co., Ltd. (Fukuoka, Japan).

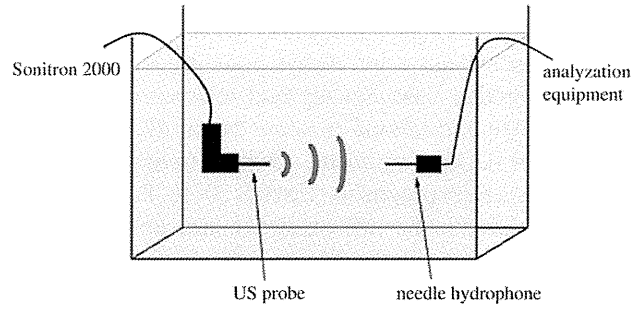

Schema 1. The simplified schema of the measurement system to evaluate the output level of US. Measurement system using a needle hydrophone in a water tank to assess and compute some acoustic parameters of Sonitron 2000 with a 3 and 6 mm unfocused probes.

Induction of intracameral fibrin clot formation and evaluation. In each of the following procedures, Brown-Norway rats were anesthetized with an intramuscular injection of ketamine hydrochloride (50 mg/kg) and xylazine hydrochloride (20 mg/kg), and the ocular surface was anesthetized with a topical instillation of 0.2% oxybuprocaine hydrochloride eye drops (Santen Pharmaceutical Co., Ltd., Osaka, Japan). Intracameral bleeding was induced by a neodymium-doped yttrium aluminium garnet (Nd:YAG) laser according to previous report (Sakamoto et al. 1999). Nd:YAG laser radiation on the iris is a standard treatment in clinical ophthalmology for glaucoma and appears to be a safe (Drake 1987; Tomey et al. 1987). In this study, laser radiation was performed by the Q-switched Nd:YAG laser system mounted on a slit lamp (Ellex Japan Inc., Osaka, Japan) using energy setting of 1.2 mJ per shot and single pulse mode. Nd:YAG laser were shot at six points on the iris (0, 2, 4, 6, 8 and 10 o'clock) with the spot size of 8 μm. In order to confirm the selectivity of YAG laser treatment, three eyes were enucleated immediately and fixed with 3.7% formaldehyde in phosphate buffered saline (PBS), dehydrated with a graded alcohol series and embedded in paraffin. The sections were cut and stained with hematoxylin and eosin. All of the specimens were then observed by two masked observers who received no information about the specimens. After laser shots, moderate to severe bleeding occurred immediately, clot and fibrin was discerned on the surface of the iris and lens on the next day. The value of clot formation in the anterior chamber was graded using surgical microscopy according to the previously described method (Sakamoto et al. 1999). Briefly, the criteria were defined as follows: 3+, clot or bleeding occupies more than one-third of the anterior chamber; 2+, between one-fifth and one-third of anterior chamber; 1+, less than one-fifth of anterior chamber; 0, no clot or bleeding. The eyes were observed by surgical microscopy everyday and photographs were taken on the next day (day 1) and fourth day (day 3) by masked observers.

Sonothrombolysis. The day after the laser shots, a 3 mm US probe was placed directly onto the corneal surface, coupling with a gel, hydroxyethyl cellulose (Senju Pharmaceutical Co. Ltd., Osaka, Japan) of the rats under general anesthesia and US was irradiated. The parameters of US were set at frequency of 1.0 MHz, duty cycle of 5.2%, pulse repetition frequency of 20 Hz and $I_{SPPA.3}$ of 0.228 W/cm^2 and US was irradiated for 5 min and the experimental groups were divided as follows: US alone (US group, $n = 14$), US and subconjunctival tPA (US and subconjunctival tPA group, $n = 14$), subconjunctival tPA alone (tPA group, $n = 14$) and no treatment (control, $n = 14$). When t-PA was applied, 50 μL of t-PA (2000 IU) after diluting with saline (final concentration 40 IU/μL) was injected into the center of the tarsal conjunctiva using a syringe with a 30-gauge needle under surgical microscopy. Given that tPA weights 68 kDa, subconjunctival injection of tPA would have a limited effect, however, the thrombus was dissolved even a little intracameral administration in our preliminary study. So, this method was done as a topical administration.

Ocular surface temperature and histologic findings. Brown-Norway rats were first anesthetized as described above. A 3 mm US probe was placed directly onto the corneal surface and US was irradiated under the following conditions: frequency of 1.0 MHz, high intensity mode (indicated on the device) and duty cycle of 5.2% or 100%. The temperature was monitored for 5 min using infrared thermography (TH6200R, NEC Co., Ltd., Tokyo, Japan). For the microscopic analysis, the eyes were enucleated after 48 h and were examined histologically the same way as above. More than six eyes of each group were examined.

Statistical analysis. All values were expressed as mean ± SD. Analysis of variance with paired *t*-test was used to determine the significance of the difference in a multiple comparison. Differences with a p value of less than 0.05 were considered to be significant.

RESULTS

In vitro study

US exposure time. US exposure was examined under the above conditions for 5 min or 20 min (exposure time). The results showed that D-dimer was significantly increased by US exposure and that 20 min exposure of US resulted in significantly higher levels than 5 min exposure (Fig. 1, $p < 0.01$). In this condition, there was no

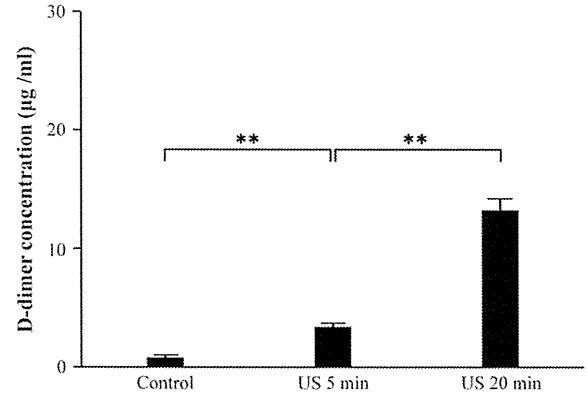

Fig. 1. Amount of D-dimer after US exposure. D-dimer increased after US exposure in a time-dependent fashion (paired *t*-test, $^{**}p < 0.01$). Control; neither US nor tPA.